NATIONAL ADVISORY COMMITTEE FOR AERONAUTICS

TECHNICAL NOTE 4397

STATIC LONGITUDINAL AND LATERAL STABILITY CHARACTERISTICS

AT LOW SPEED OF 60° SWEPTBACK-MIDWING MODELS HAVING

WINGS WITH AN ASPECT RATIO OF 2, 4, OR 6

By Walter D. Wolhart and David F. Thomas, Jr.

Langley Aeronautical Laboratory
Langley Field, Va.

NACA

Washington

September 1958

NATIONAL ADVISORY COMMITTEE FOR AERONAUTICS

TECHNICAL NOTE 4397

STATIC LONGITUDINAL AND LATERAL STABILITY CHARACTERISTICS

AT LOW SPEED OF 60° SWEPTBACK-MIDWING MODELS HAVING

WINGS WITH AN ASPECT RATIO OF 2, 4, OR 6

By Walter D. Wolhart and David F. Thomas, Jr.

SUMMARY

A systematic investigation was performed in the Langley stability tunnel to determine the static longitudinal and lateral stability characteristics at low speed of a series of 60° sweptback-midwing models having wings with an aspect ratio of 2, 4, or 6. Although both static longitudinal and lateral stability data are presented, emphasis has been placed on the contribution of the various components and combinations of components to directional stability at high angles of attack. Also included are some comparisons with the directional stability characteristics of similar unswept- and 45° sweptback-wing configurations.

The results show that all 60° sweptback-wing complete model configurations become directionally unstable in the moderate to high angle-of-attack range. This loss in directional stability can be attributed to the large unstable contribution of the wing-fuselage combination and to the decrease in tail contribution with increasing angle of attack. The decrease in tail contribution with increasing angle of attack is attributed to the effective increase in sweep angle of the vertical tail with increasing angle of attack and to adverse fuselage interference at the tail. In general, the tail contribution to directional stability at high angles of attack decreased with increasing wing aspect ratio either with or without the fuselage.

A comparison of the results for the 60° sweptback-wing models with results for similar unswept- and 45° sweptback-wing models indicates that for these configurations increasing sweepback increases the likelihood of directional instability at high angles of attack. Although comparable losses in the tail contribution to directional stability with increasing angle of attack were noted for all wing sweep angles, there was a compensating shift in the contribution of the unswept-wing—fuselage combination that was not present for the 45° and 60° sweptback-wing configurations.

INTRODUCTION

Recent advances in understanding the principles of high-speed flight have led to significant changes in the design of the principal components of airplanes. Among the more noticeable and important of these changes have been the trend to low-aspect-ratio swept wings and the general concentration of the weight of the airplane along the fuselage. These changes to the basic geometry of airplanes have brought about certain characteristics, both aerodynamic and inertial, which may result in a configuration that is susceptible to large inadvertent motions. These motions may result in the attainment of large angles of attack and sideslip from which ensuing stalls and spins appear to be more likely than with previous configurations. One of the important aerodynamic deficiencies of some present-day airplanes, which contribute to such undesirable motions, is the loss of directional stability at moderate and high angles of attack.

In general, the directional stability as well as the other aerodynamic characteristics of midwing or near midwing models can be estimated satisfactorily at low angles of attack by various theoretical and empirical methods such as those presented in reference 1. The results at moderate and high angles of attack, however, are oftentimes unreliable because of the unpredictable interference effects of the various components. Considerable information is available on the influence of the wing, fuselage, and tail geometry on the static stability characteristics of airplanes with either unswept or swept wings. However, little information of a systematic nature is available on the effects of wing aspect ratio and sweep on the contribution of the various components of the complete model.

In order to provide such information, a series of experimental investigations have been performed in the Langley stability tunnel using models having various interchangeable components and having wings of aspect ratio 2, 4, or 6. The results of these investigations for unswept and 45° sweptback wings are presented in references 2 and 3, respectively, and the results for 60° sweptback wings are presented herein. Although both static longitudinal and lateral stability data are presented, emphasis has been placed on the directional stability at high angles of attack.

The models used in the present investigation were tested through an angle-of-attack range from approximately -4° to 32°. The lateral stability derivatives were determined from tests made at angles of sideslip of 5° and -5°, although a few configurations using the aspect-ratio-4 wing were tested through a large sideslip range from -20° to 20° for several angles of attack.

SYMBOLS

The data presented herein are referred to the stability system of axes with the origin at the projection on the plane of symmetry of the quarter-chord point of the wing mean aerodynamic chord. Positive directions of forces, moments, and angular displacements are shown in figure 1. The coefficients and symbols are defined as follows:

A aspect ratio, b^2/S

b span, ft

C_D' approximate drag coefficient, $\dfrac{\text{Approximate drag}}{qS_W}$

C_L lift coefficient, $\dfrac{\text{Lift}}{qS_W}$

C_l rolling-moment coefficient, $\dfrac{\text{Rolling moment}}{qS_W b_W}$

C_m pitching-moment coefficient, $\dfrac{\text{Pitching moment}}{qS_W \bar{c}_W}$

C_n yawing-moment coefficient, $\dfrac{\text{Yawing moment}}{qS_W b_W}$

C_Y side-force coefficient, $\dfrac{\text{Side force}}{qS_W}$

$C_{l_\beta} = \dfrac{\partial C_l}{\partial \beta}$

$C_{n_\beta} = \dfrac{\partial C_n}{\partial \beta}$

$C_{Y_\beta} = \dfrac{\partial C_Y}{\partial \beta}$

c local chord, ft

$\bar{c}$ mean aerodynamic chord, $\dfrac{2}{S}\displaystyle\int_0^{b/2} c^2 dy$, ft

l tail length, distance measured parallel to fuselage reference line from moment reference to $\bar{c}/4$ of the tail, ft

q free-stream dynamic pressure, $\frac{1}{2}\rho V^2$, lb/sq ft

r ordinate of circular fuselage, in.

S area, sq ft

V free-stream velocity, ft/sec

x longitudinal distance from fuselage nose measured parallel to fuselage reference line, in.

y spanwise distance measured from and perpendicular to plane of symmetry, ft

$\bar{y}$ spanwise distance to mean aerodynamic chord, measured from and perpendicular to plane of symmetry, $\frac{2}{S}\int_0^{b/2} cy\ dy$, ft

α angle of attack, deg

β angle of sideslip, deg

Λ sweepback angle of wing quarter-chord line, deg

ρ density, slugs/cu ft

Subscripts:

h horizontal tail

r root

t tip

VH contribution of vertical-tail—horizontal-tail assembly to various force and moment coefficients

v vertical tail

w wing

WF contribution of wing and fuselage

$WFVH$ contribution of complete model

Model component designations:

W   wing alone

F   fuselage alone

VH   combination of vertical and horizontal tail, always tested as
           a unit (tail alone)

WF   wing-fuselage combination

WVH   wing-tail combination

FVH   fuselage-tail combination

WFVH   wing-fuselage-tail combination (complete model)

The contribution of the vertical-tail—horizontal-tail assembly to
the various force and moment coefficients is obtained by subtracting the
data of various configurations as follows:

FVH-F   fuselage-tail combination minus fuselage alone

WVH-W   wing-tail combination minus wing alone

WFVH-WF   complete model minus wing-fuselage combination

APPARATUS AND MODELS

This investigation was performed in the 6-foot-diameter test section
of the Langley stability tunnel. The models were mounted on a single
strut support which was in turn fastened to a conventional six-component
electromechanical balance system.

The models used in this investigation were constructed primarily
of laminated mahogany and consisted of three 60° sweptback wings of
aspect ratios 2, 4, and 6, a fuselage of fineness ratio 7.50, and
60° sweptback vertical and horizontal tails of aspect ratios 0.90
and 1.79, respectively. The wing and tail surfaces had NACA 65A008 air-
foil sections and a taper ratio of 0.6. Geometric characteristics of
the various components are given in figures 2 and 3 and tables I and II.
Since appreciable bending and twist might be expected for the wings of
aspect ratio 4 and 6 if constructed only of mahogany, these wings were
constructed with 1/16-inch-thick Inconel and aluminum-alloy stiffeners
cycle-welded in place near the upper and lower surfaces of the wing.

In general, the models were designed to permit testing of the individual components as well as various combinations of components. The only exceptions were the vertical and horizontal tails which were not separable and were always tested as a unit. For the wing-tail configurations the tails were mounted at the appropriate tail length on a small-diameter steel tube which was in turn fastened to the wing. The isolated tails were mounted on the same tube which was fastened to the model support strut.

TESTS AND CORRECTIONS

All the tests were made at a dynamic pressure of 24.9 pounds per square foot which corresponds to a Mach number of 0.13. The Reynolds numbers based on the mean aerodynamic chord of the various wings were 1.02×10^6 for the aspect-ratio-2 wing, 0.72×10^6 for the aspect-ratio-4 wing, and 0.59×10^6 for the aspect-ratio-6 wing. The basic static longitudinal and lateral stability characteristics were determined for an angle-of-attack range from approximately $-4°$ to $32°$. The static lateral stability derivatives were determined from tests made at angles of sideslip of $5°$ and $-5°$ and, in addition, several configurations were tested through a sideslip range from $-20°$ to $20°$ for several angles of attack.

Approximate jet-boundary corrections were applied to the data by the method of reference 4. Pitching-moment coefficients for the configurations with horizontal tail on were corrected for the effect of the jet boundaries by the method of reference 5. Tare corrections have been applied only to the wing-on basic longitudinal data C_L, C_m, and C_D'.

The data have not been corrected for the effects of blockage since these corrections are considered negligible. No aeroelastic corrections have been applied to the data; however, calculations to determine the magnitude of these corrections indicate that they are negligible for the dynamic pressure of these tests.

PRESENTATION OF RESULTS

The results of this investigation are presented as force and moment coefficients and derivatives plotted against angle of attack or sideslip for the various model configurations. (See figs. 4 to 24.) A summary of the configurations investigated and of the figures that present data for these configurations, together with the purpose of these figures, is given in table III.

DISCUSSION

In general, the discussion of the results of this investigation will be confined to the directional stability characteristics with emphasis on the contribution of the various components at high angles of attack. It should be pointed out that comparing moment coefficients for configurations where wing aspect ratio is the only variable can be somewhat misleading since the characteristic lengths $\bar{c}_w$ and b_w on which the coefficients are based change with changes in wing aspect ratio. This change in the characteristic length results in a given moment being transformed into different coefficients for each aspect ratio. Examples of the possible misinterpretation of data may be noted in figures 5 and 14, wherein data are presented for the wing-off configurations for the three different aspect ratios. In order to eliminate this apparent effect of wing aspect ratio on the tail contribution to directional stability $C_{n_\beta, VH}$, figure 23 has been prepared in which the tail length l is used in place of b_w as the characteristic dimension. The force coefficients are directly comparable, however, since the wing area remained constant for all wing aspect ratios.

Static Longitudinal Stability Characteristics

The basic static longitudinal stability data which show the variation of C_L, C_D', and C_m with α for the various components and combinations of components are presented in figures 4 and 5 for wing-on and wing-off configurations, respectively. In general, all wing-on configurations show an increase in lift-curve slope and a rapid increase in drag at the angle of attack at which nonlinearities occur in the pitching-moment curves. Since the characteristics shown are typical of sweptback wings which have been rather extensively investigated previously, there is little need to discuss them in detail here.

It is interesting to note that the unstable contribution of the fuselage alone to pitching moment is canceled to a large extent by mutual interference of the wing and fuselage when the fuselage is tested in combination with any of the wings either with the tail on or the tail off. (See figs. 4 and 5.)

The variation of C_L and C_m with β at several angles of attack for the aspect-ratio-4 wing and various components and combinations of components is presented in figures 6 to 12. The trends shown for the wing-alone or wing-fuselage combination are in qualitative agreement with the results for the high Reynolds number investigation reported in reference 6. However, the nonlinearities in the lift and pitching-moment

curves are delayed to somewhat larger angles of attack and sideslip for
the high Reynolds number.

Lateral Stability Characteristics

Basic static lateral stability characteristics.- The basic static
lateral stability data which show the variation of C_{Y_β}, C_{n_β}, and C_{l_β}
with α for various components and combinations of components are pre-
sented in figures 13 and 14 for wing-on and wing-off configurations,
respectively. In general, these data show that all complete model con-
figurations become directionally unstable in the moderate to high angle-
of-attack range. This loss in directional stability may be attributed
to an increase in the unstable contribution of the wing-fuselage com-
bination and to a decrease in tail contribution with increasing angle of
attack. The initial unstable break in the directional stability curves
at an angle of attack of about 8° for configurations involving the
aspect-ratio-4 and, to some extent, the aspect-ratio-6 wing is attributed
to an abrupt loss in leading-edge suction on the trailing wing panel of
the sideslipped wing. The increase in the unstable contribution of the
fuselage for the aspect-ratio-2 wing-fuselage combination at high angles
of attack is believed to be associated with wing-induced sidewash on the
fuselage afterbody (ref. 7). This adverse wing-sidewash effect decreases
with increasing wing aspect ratio and, in fact, for the aspect-ratio-6
wing-fuselage combination the sidewash has a slight favorable effect.

The data also show that at moderate and high angles of attack the
fuselage, when tested in combination with the aspect-ratio-6 wing, has
a large effect on the effective dihedral derivative C_{l_β}. Apparently
the fuselage is altering the span loading on the wing since the fuselage
alone contributes very little to C_{l_β}. (See fig. 14.) The fuselage has
very little effect on C_{l_β} for configurations employing the aspect-ratio-2
or aspect-ratio-4 wing.

Since these data were obtained at a relatively low Reynolds number
and since it is well known that increases in Reynolds number may have an
appreciable effect on the static stability characteristics, particularly
on the wing contribution, some consideration should be given to Reynolds
number effects. No high Reynolds number data were obtained in this
investigation; however, some indication of effects to be expected from
increases in Reynolds number can be obtained from other high Reynolds num-
ber investigations. For example, reference 8 shows that increasing the
Reynolds number from 1.2×10^6 to 4.45×10^6 had no appreciable effect
on the directional stability characteristics of a complete model con-
figuration having a 45° sweptback wing of aspect ratio 6 but did delay

the initial break in the C_{l_β} curve to a higher angle of attack. In addition, some recent data obtained from tests on a 45° sweptback-wing model of aspect ratio 4 and having NACA 65A006 airfoil indicated that increasing the Reynolds number from 0.7×10^6 to 7.1×10^6 delayed the initial break in the C_{l_β} curve from about 4° to 10° but had little effect on either C_{n_β} or C_{l_β} for angles of attack above about 12°. Therefore, although the low Reynolds number data presented herein would probably be in poor quantitative agreement with high Reynolds number data in the low to moderate angle-of-attack range, the trends are believed to be reliable and at high angles of attack the quantitative agreement would probably be good.

The variations of C_Y, C_n, and C_l with β at several angles of attack give an indication of the range of sideslip angles for which the sideslip derivatives determined from $\beta = 5^\circ$ and -5° are applicable. (See figs. 15 to 21.) The data are for the various components and combinations of components employing the aspect-ratio-4 wing. In general, the curves are fairly linear with sideslip angle for sideslip angles between 5° and -5° for the angles of attack of approximately 0°, 10°, and 20°; therefore, the sideslip derivatives obtained from pitch tests at $\beta = 5^\circ$ and -5° should be representative.

Tail contribution.- The tail contribution to directional stability $C_{n_\beta,VH}$, as well as to the other sideslip derivatives, was obtained by subtracting the results for tail-off configurations from the results for tail-on configurations. For example, in equation form:

$$C_{n_\beta,VH} = C_{n_\beta,WFVH} - C_{n_\beta,WF}$$

These tail contributions are presented as a function of angle of attack in figures 22.

The data presented in figure 22(b) show that the decrease in the tail contribution to directional stability with increasing angle of attack for the complete model can be largely attributed to two factors. One factor is the decreased contribution of the isolated vertical tail which can at least in part be attributed to the effective increase in sweepback of the vertical tail with increasing angle of attack. The other factor is the adverse fuselage interference or blanketing effect at the tail.

As might be expected, the separate effects of the wing and fuselage interference on the tail contribution are modified somewhat for the

complete model configuration. The results indicate that the interference at the tail for angles of attack up to about 22° is slightly less adverse for the complete model than would be obtained by adding the separate effects of the wing and fuselage. The favorable effect noted when the wing is added to the fuselage is attributed to a reduction in adverse effects resulting from the downward displacement of the fuselage vortex.

A direct measure of the effect of wing aspect ratio on the tail contribution to directional stability is provided in figure 23 which shows the variation of $\frac{b_W}{l} C_{n_\beta,VH}$ with α. This figure provides a comparison between the wing-on and wing-off tail contribution both with and without the fuselage. In general, these data show that the tail contribution to directional stability at high angles of attack decreases with increasing wing aspect ratio either with or without the fuselage. It should be pointed out however that the effects of changes in wing aspect ratio on the tail contribution to directional stability are probably minimized for the complete model configurations by the large fuselage effect mentioned previously.

Effects of Sweepback on Directional Stability

The effects of sweepback on the directional stability characteristics of configurations with wings of aspect ratio 2, 4, or 6 are indicated by figure 24. (Unswept-wing data were obtained from ref. 2 and 45° sweptback-wing data from ref. 3.) Figure 24(a) shows the effect of wing sweepback on the wing-fuselage contribution to directional stability for various wing aspect ratios. The tail contribution to directional stability, when in the presence of the fuselage, has been normalized by dividing by the value at 0° angle of attack and these results are presented in figures 24(b) and 24(c) for wing-on and wing-off configurations, respectively. Since configurations involving the aspect-ratio-2 wing exhibited aerodynamic hysteresis in sideslip for angles of attack above about 20°, a dashed line has been used to distinguish this region. (See ref. 2.)

The data of figure 24 show that for these configurations increasing wing sweepback increases the likelihood of directional instability at high angles of attack because of decreased tail contribution and the large unstable contribution of the wing-fuselage combination. At high angles of attack, comparable losses in tail contribution are shown for all sweep angles, but for the unswept configurations there is a compensating stable shift in the wing-fuselage contribution. The tail contribution to directional stability decreased at high angles of attack because of large adverse sidewash effects which for the unswept-wing and 45° sweptback-wing models were primarily due to the wing and which for the 60° sweptback-wing models were primarily due to the fuselage. The

relative effects of wing sweepback on the tail contribution to directional stability are difficult to evaluate from these data since these effects are no doubt influenced by the fact that for these configurations the tail aspect ratio decreased with increasing sweepback. (See refs. 2 and 3.)

CONCLUSIONS

An experimental investigation was made to determine the static longitudinal and lateral stability characteristics at low speed of 60° sweptback-midwing models having wings with an aspect ratio of 2, 4, or 6. The results of the investigation indicate the following conclusions:

1. All 60° sweptback-wing complete model configurations became directionally unstable in the moderate to high angle-of-attack range, and this can be attributed to the large unstable contribution of the wing-fuselage combination and to the decrease in vertical-tail contribution with increasing angle of attack. The decrease in tail contribution with increasing angle of attack is attributed to the effective increase in sweep angle of the vertical tail with increasing angle of attack and to adverse fuselage interference at the tail.

2. In general, the tail contribution to directional stability at high angles of attack decreased with increasing wing aspect ratio either with or without the fuselage.

3. Comparison of results for the 60° sweptback-wing models with results for similar unswept-wing and 45° sweptback-wing models indicates that for these configurations increasing sweepback increases the likelihood of directional instability at high angles of attack. Although comparable losses in the tail contribution to directional stability were noted for all wing sweep angles, there was a compensating stable shift in the contribution of the unswept-wing—fuselage combination that was not present for the 45° and 60° sweptback-wing models.

Langley Aeronautical Laboratory,
        National Advisory Committee for Aeronautics,
                Langley Field, Va., July 21, 1958.

REFERENCES

1. Campbell, John P., and McKinney, Marion O.: Summary of Methods for
     Calculating Dynamic Lateral Stability and Response and for Estimating
     Lateral Stability Derivatives. NACA Rep. 1098, 1958. (Supersedes
     NACA TN 2409.)

2. Wolhart, Walter D., and Thomas, David F., Jr.: Static Longitudinal
     and Lateral Stability Characteristics at Low Speed of Unswept-
     Midwing Models Having Wings With an Aspect Ratio of 2, 4, or 6.
     NACA TN 3649, 1956.

3. Thomas, David F., Jr., and Wolhart, Walter D.: Static Longitudinal
     and Lateral Stability Characteristics at Low Speed of 45° Sweptback-
     Midwing Models Having Wings With an Aspect Ratio of 2, 4, or 6.
     NACA TN 4077, 1957.

4. Silverstein, Abe, and White, James A.: Wind-Tunnel Interference With
     Particular Reference to Off-Center Positions of the Wing and to the
     Downwash at the Tail. NACA Rep. 547, 1936.

5. Gillis, Clarence L., Polhamus, Edward C., and Gray, Joseph L., Jr.:
     Charts for Determining Jet-Boundary Corrections for Complete Models
     in 7- by 10-Foot Closed Rectangular Wind Tunnels. NACA WR L-123,
     1945. (Formerly NACA ARR L5G31.)

6. McCormack, Gerald M., and Walling, Walter C.: Aerodynamic Study of
     a Wing-Fuselage Combination Employing a Wing Swept Back 63°. -
     Investigation of a Large-Scale Model at Low Speed. NACA RM A8D02,
     1949.

7. Polhamus, Edward C., and Spreemann, Kenneth P.: Subsonic Wind-Tunnel
     Investigation of the Effect of Fuselage Afterbody on Directional
     Stability of Wing-Fuselage Combinations at High Angles of Attack.
     NACA TN 3896, 1956.

8. Griner, Roland F.: Static Lateral Stability Characteristics of an
     Airplane Model Having a 47.7° Sweptback Wing of Aspect Ratio 6 and
     the Contribution of Various Model Components at a Reynolds Number
     of 4.45×10^6. NACA RM L53G09, 1953.

TABLE I.- GEOMETRIC CHARACTERISTICS OF MODELS

Fuselage:
  Length, ft 3.75
  Fineness ratio 7.50

Wings:

Aspect ratio	2	4	6
Quarter-chord sweep angle, deg	60	60	60
Dihedral angle, deg	0	0	0
Twist, deg	0	0	0
Airfoil section	NACA 65A008	NACA 65A008	NACA 65A008
Area, sq ft	2.250	2.250	2.250
Span, ft	2.122	3.000	3.675
Mean aerodynamic chord, ft	1.083	0.766	0.625
Root chord, ft	1.326	0.938	0.765
Taper ratio	0.6	0.6	0.6

Vertical tail:
  Aspect ratio 0.9
  Quarter-chord sweep angle, deg 60
  Airfoil section . . . . NACA 65A008
  Area, sq ft 0.338
  Span, ft 0.550
  Mean aerodynamic chord, ft 0.626
  Root chord, ft 0.767
  Taper ratio 0.6
  Ratio of tail area to wing area 0.150
  Tail length, distance measured parallel to fuselage
    reference line from moment reference to $\bar{c}/4$ of
    tail, ft 1.392

Horizontal tail:
  Aspect ratio 1.790
  Quarter-chord sweep angle, deg 60
  Incidence, deg 0
  Airfoil section . . . . NACA 65A008
  Area, sq ft 0.450
  Mean aerodynamic chord, ft 0.512
  Root chord, ft 0.627
  Taper ratio 0.6
  Ratio of tail area to wing area 0.200
  Tail length, distance measured parallel to fuselage
    reference line from moment reference to $\bar{c}/4$ of
    tail, ft 1.392

TABLE II.- COORDINATES OF THE

CIRCULAR-CROSS-SECTION FUSELAGE
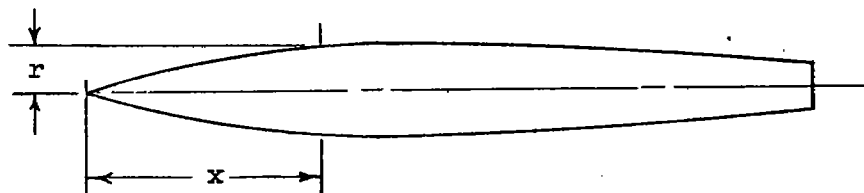
x, in.	r, in.
0	0
2.00	.64
4.00	1.20
6.00	1.68
8.00	2.09
10.00	2.42
12.00	2.67
14.00	2.85
16.00	2.96
18.00	3.00
20.00	2.99
22.00	2.97
24.00	2.93
26.00	2.87
28.00	2.79
30.00	2.70
32.00	2.60
34.00	2.47
36.00	2.33
38.00	2.18
40.00	2.01
42.00	1.82
44.00	1.61
45.00	1.50

TABLE III.- FIGURE INDEX FOR PLOTTED DATA

Data	Configuration	Figure	Purpose of figure to show -
C_L, C_D', C_m plotted against α	W, WF, WVH, WFVH	4	Effect of various model components singly and in combination on the basic longitudinal data.
	F, VH, FVH.	5	
C_L and C_m plotted against β	WFVH	6	Effect of sideslip on longitudinal stability characteristics of various components singly and in combination. $A_W = 4$.
	WF	7	
	WVH	8	
	W	9	
	FVH	10	
	F	11	
	VH	12	
C_{Y_β}, C_{n_β}, C_{l_β} plotted against α	W, WF, WVH, WFVH	13	Effect of various model components singly and in combination on static lateral derivatives.
	F, VH, FVH	14	
C_Y, C_n, C_l plotted against β	WFVH	15	Effect of sideslip on lateral stability characteristics of various components singly and in combination. $A_W = 4$.
	WF	16	
	WVH	17	
	W	18	
	FVH	19	
	F	20	
	VH	21	
$C_{Y_{\beta,VH}}$, $C_{n_{\beta,VH}}$, and $C_{l_{\beta,VH}}$ plotted against α	VH, FVH-F, WVH-W, WFVH-WF	22	Effect of various model components on the tail contribution to the static lateral derivatives.
$\frac{b_W}{l} C_{n_{\beta,VH}}$ plotted against α	VH, WVH-W, FVH-F, WFVH-WF	23	Effect of wing aspect ratio on tail contribution to directional stability with and without fuselage.
$C_{n_{\beta,WF}}$, and $\dfrac{C_{n_{\beta,VH}}}{\left(C_{n_{\beta,VH}}\right)_{\alpha=0^\circ}}$ plotted against α	WF, WFVH-WF, FVH-F	24	Effect of sweepback on wing-fuselage contribution to directional stability and rate of change of tail contribution to directional stability with angle of attack with and without the wing.
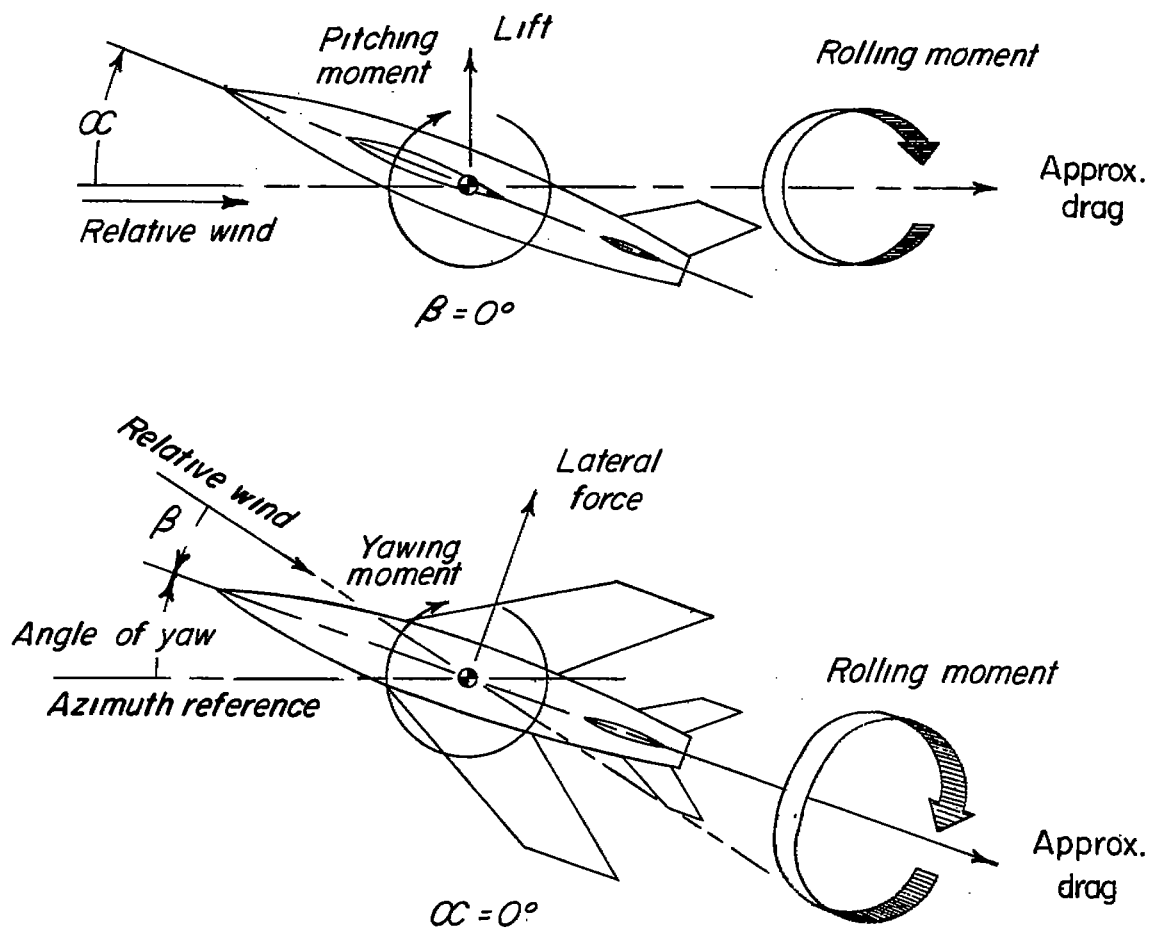
Figure 1.- System of axes used. Arrows indicate positive direction of forces, moments, and angular displacements.
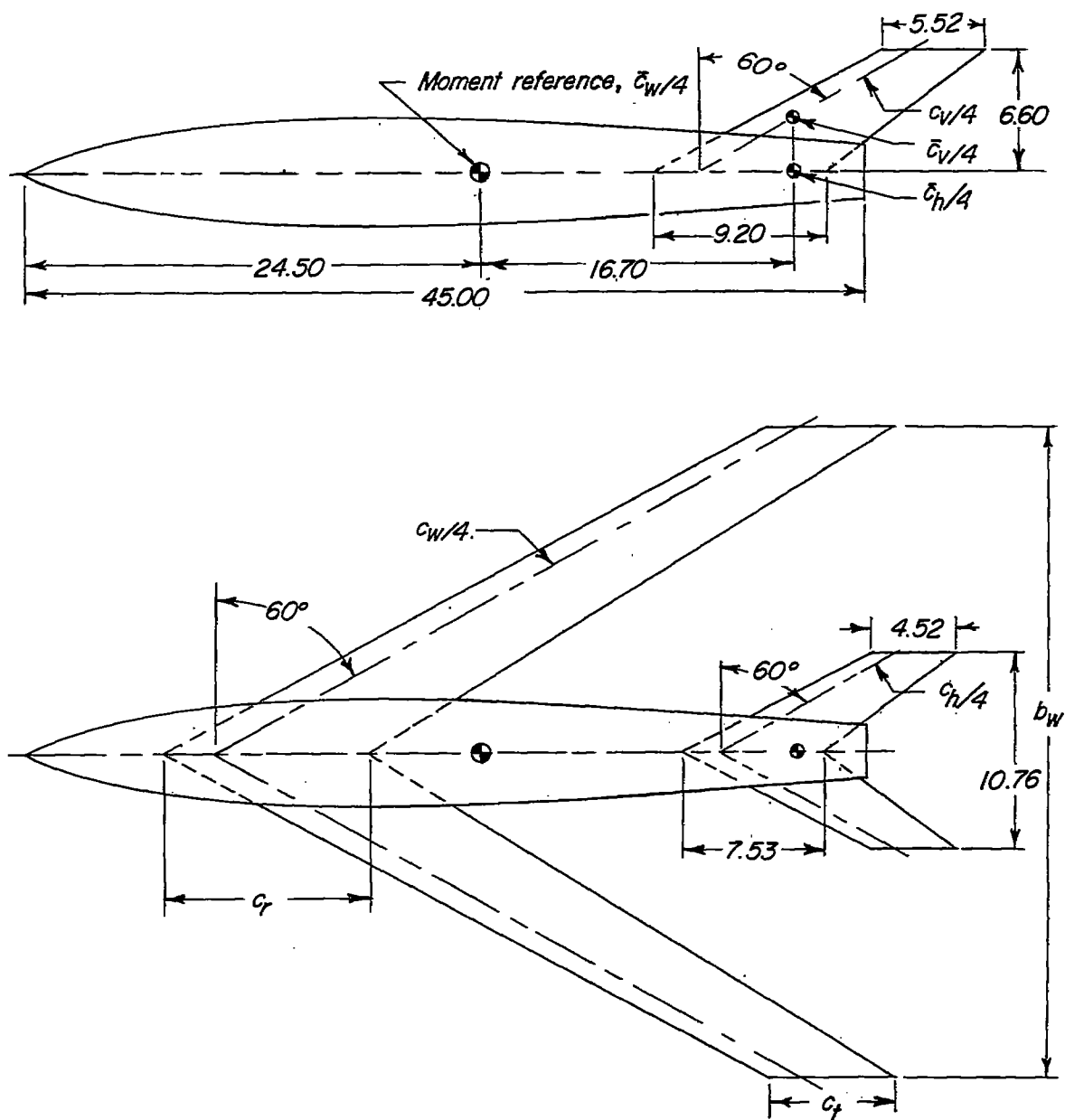
Figure 2.- General arrangement of complete models. All dimensions are in inches.
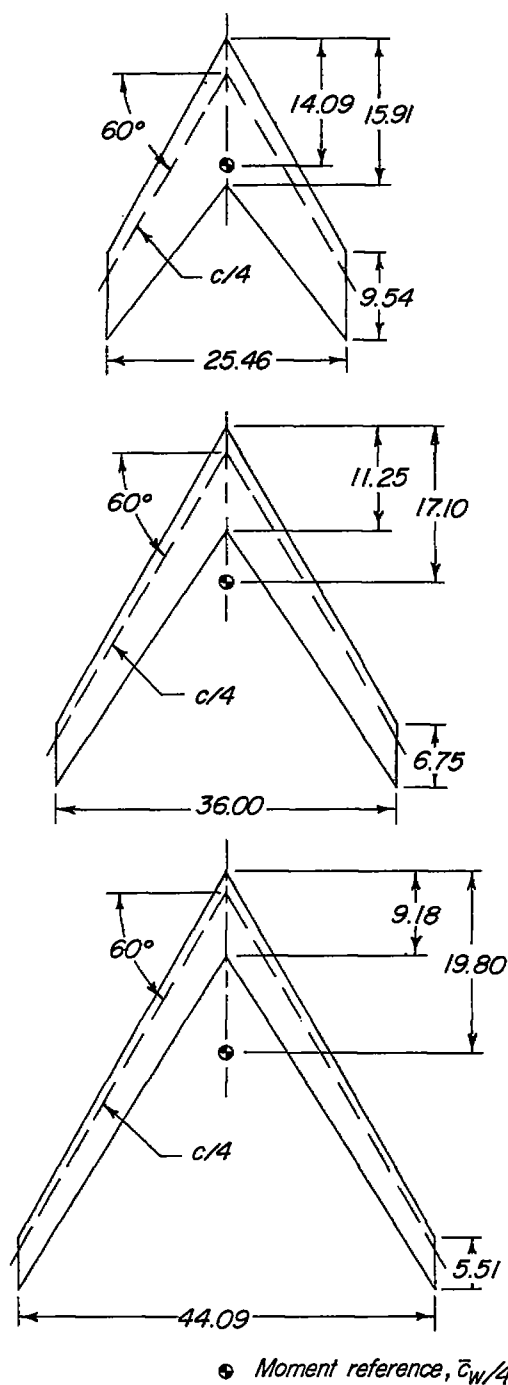
Figure 3.- Geometric characteristics of wings. All dimensions are in inches.
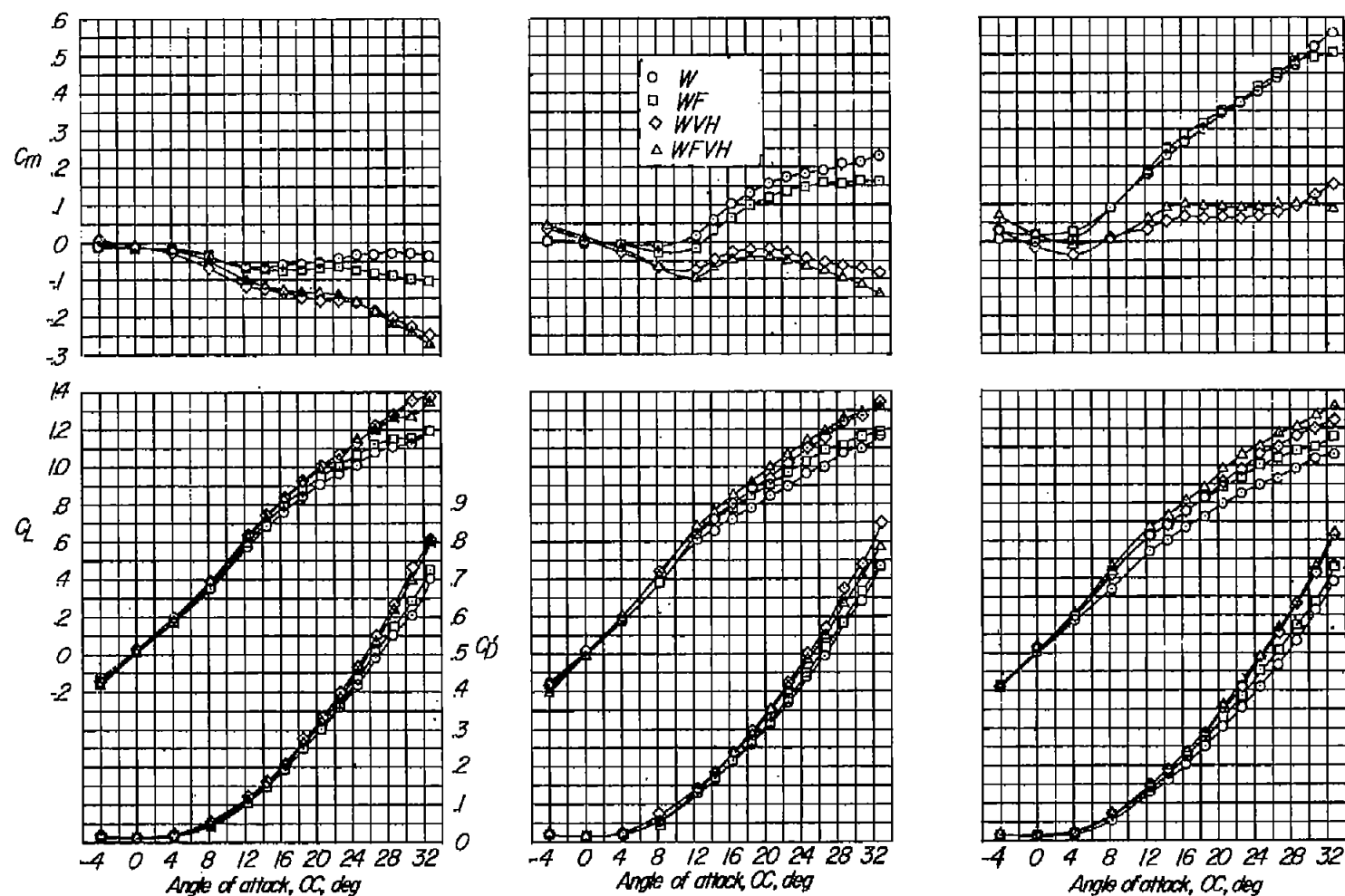
(a) Aspect-ratio-2 wing. (b) Aspect-ratio-4 wing. (c) Aspect-ratio-6 wing.

Figure 4.- Static longitudinal stability characteristics of the wing alone and in various combinations with the fuselage and tails.

(a) Coefficients based on aspect-ratio-2 wing.

(b) Coefficients based on aspect-ratio-4 wing.

(c) Coefficients based on aspect-ratio-6 wing.
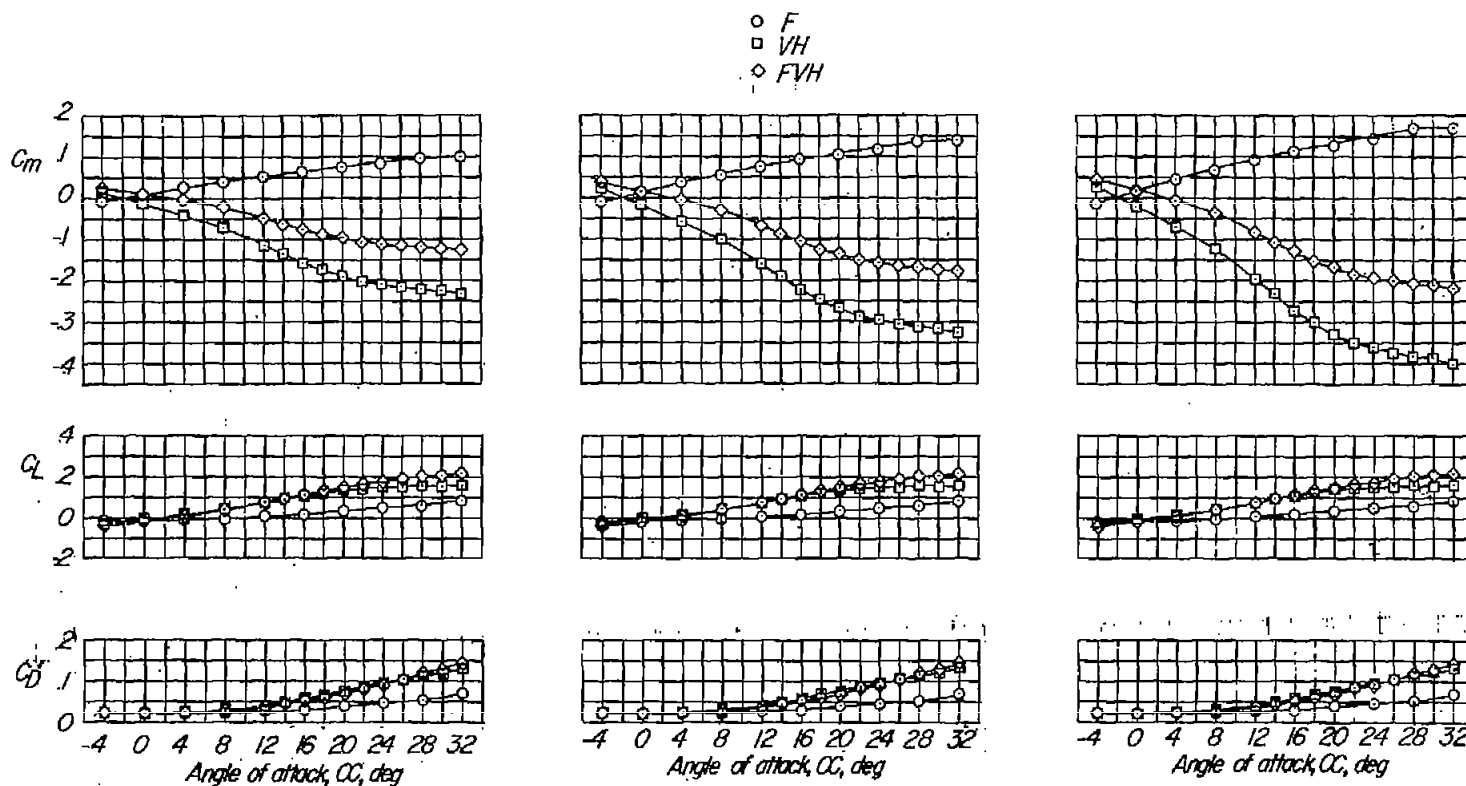
Figure 5.- Static longitudinal stability characteristics of the fuselage alone, tail alone, and fuselage-tail combination.
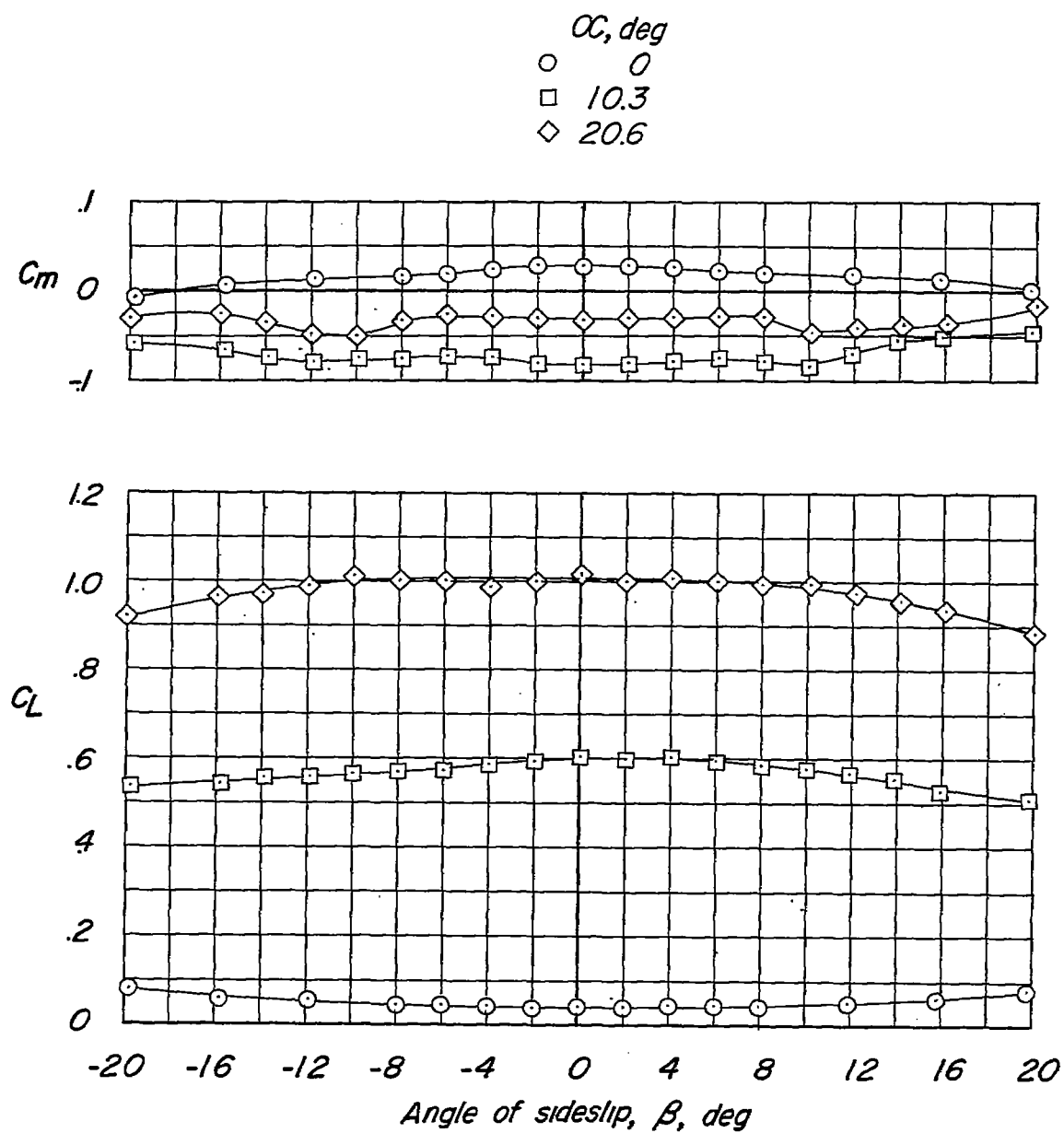
Figure 6.- Variation of C_L and C_m with β for the complete model. $A_W = 4$.
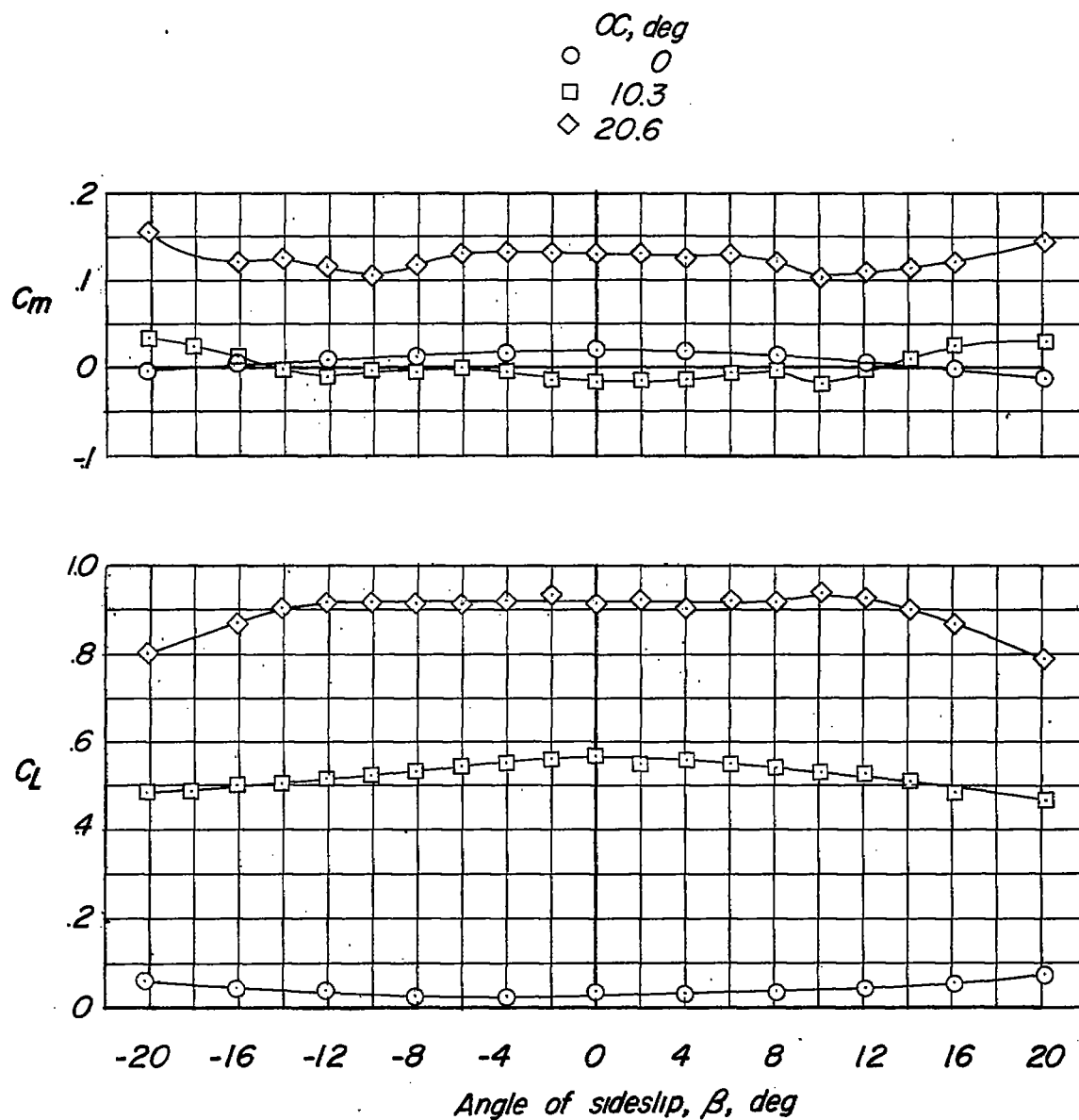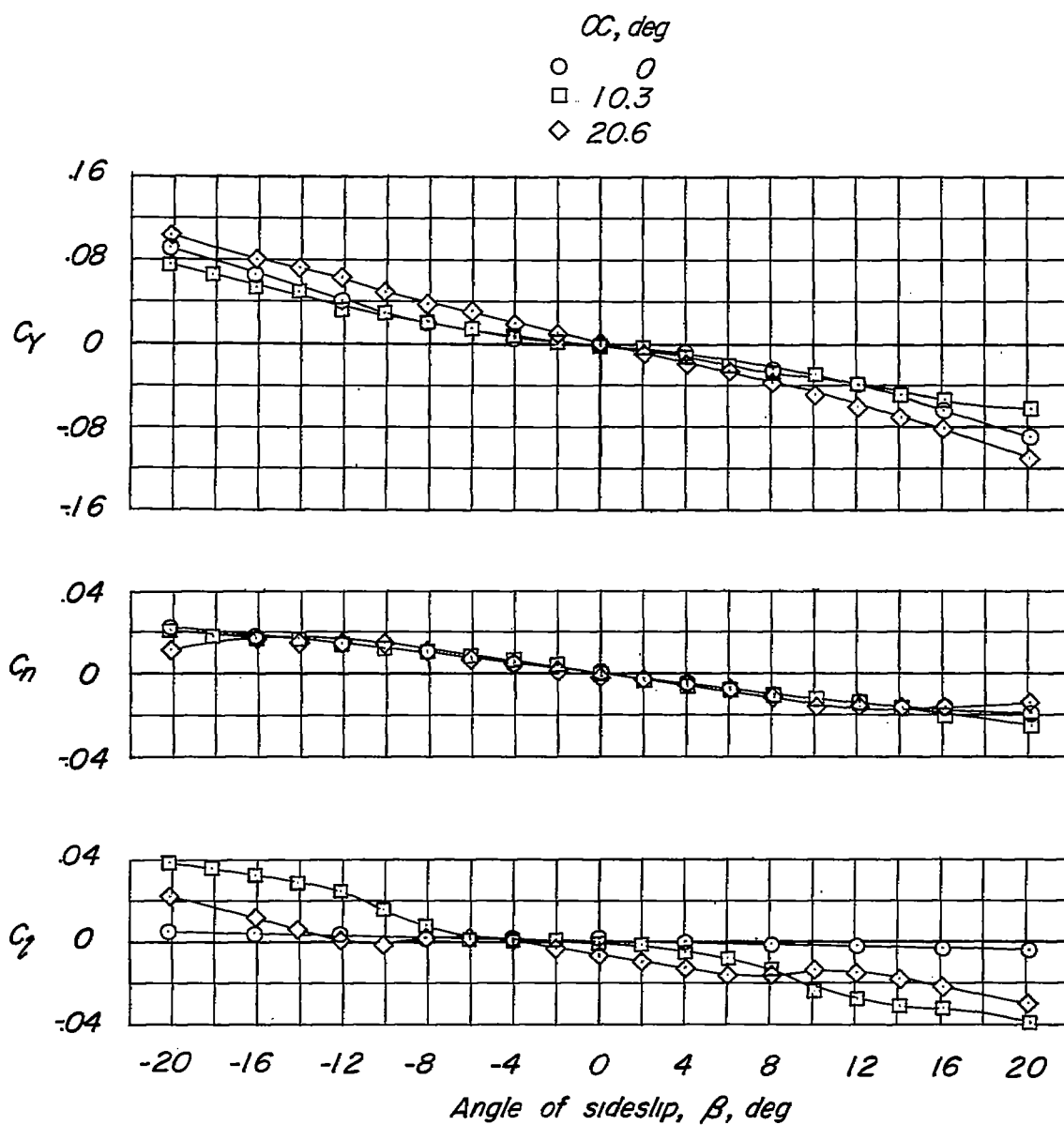
Figure 7.- Variation of C_L and C_m with β for the wing-fuselage combination. $A_w = 4$.
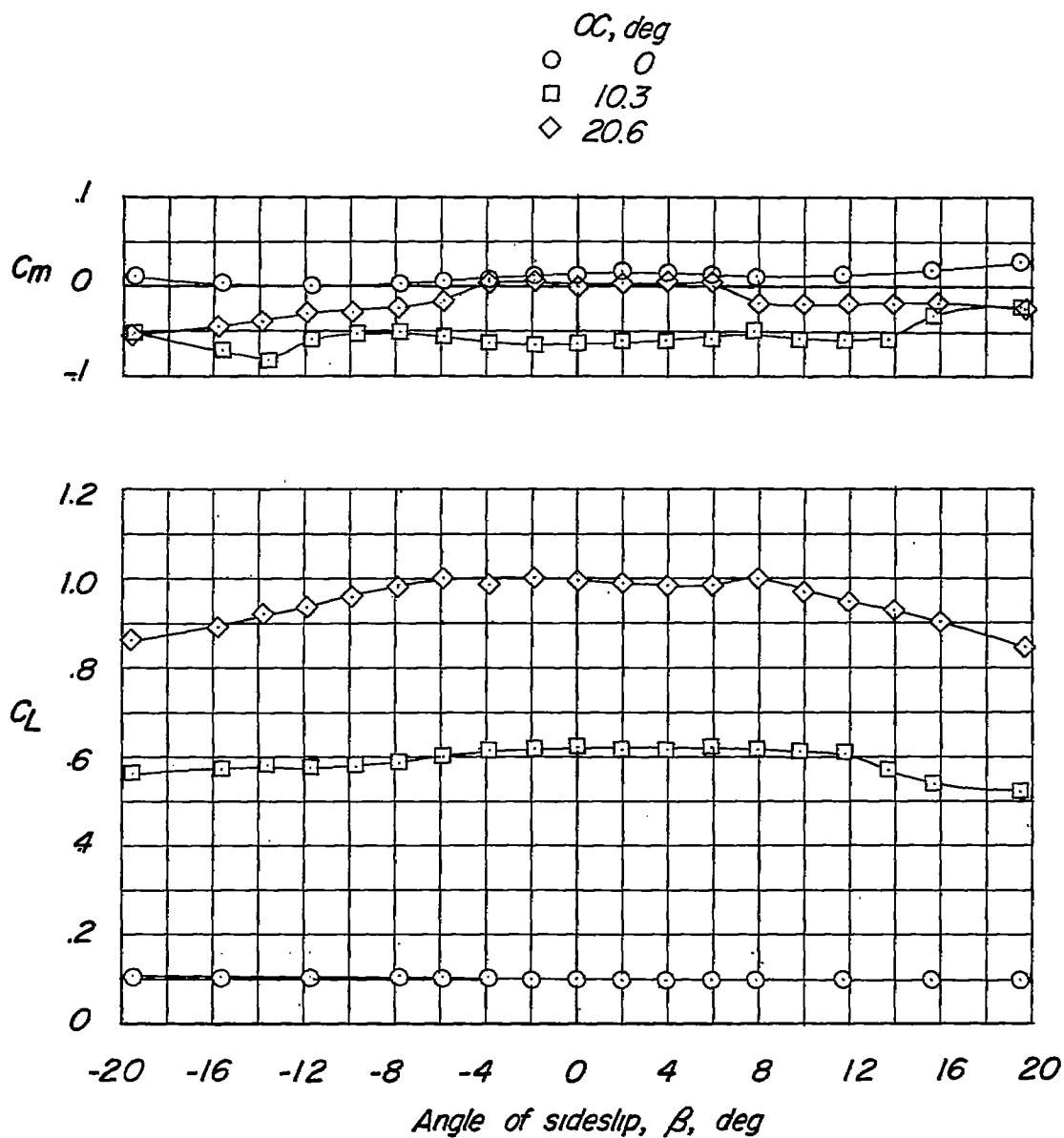
Figure 8.- Variation of C_L and C_m with β for the wing-tail combination. $A_w = 4$.
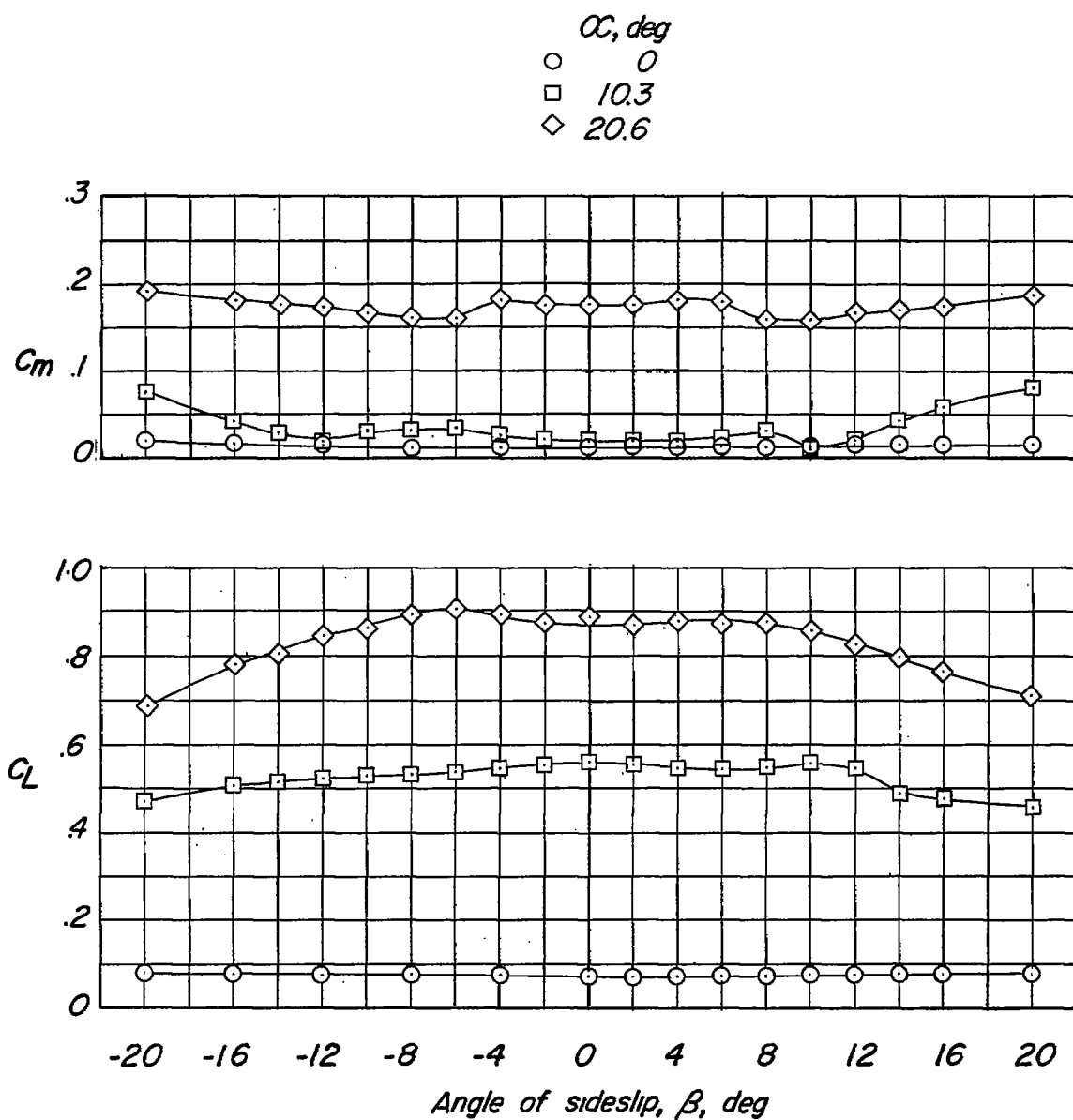
Figure 9.- Variation of C_L and C_m with β for the wing alone.
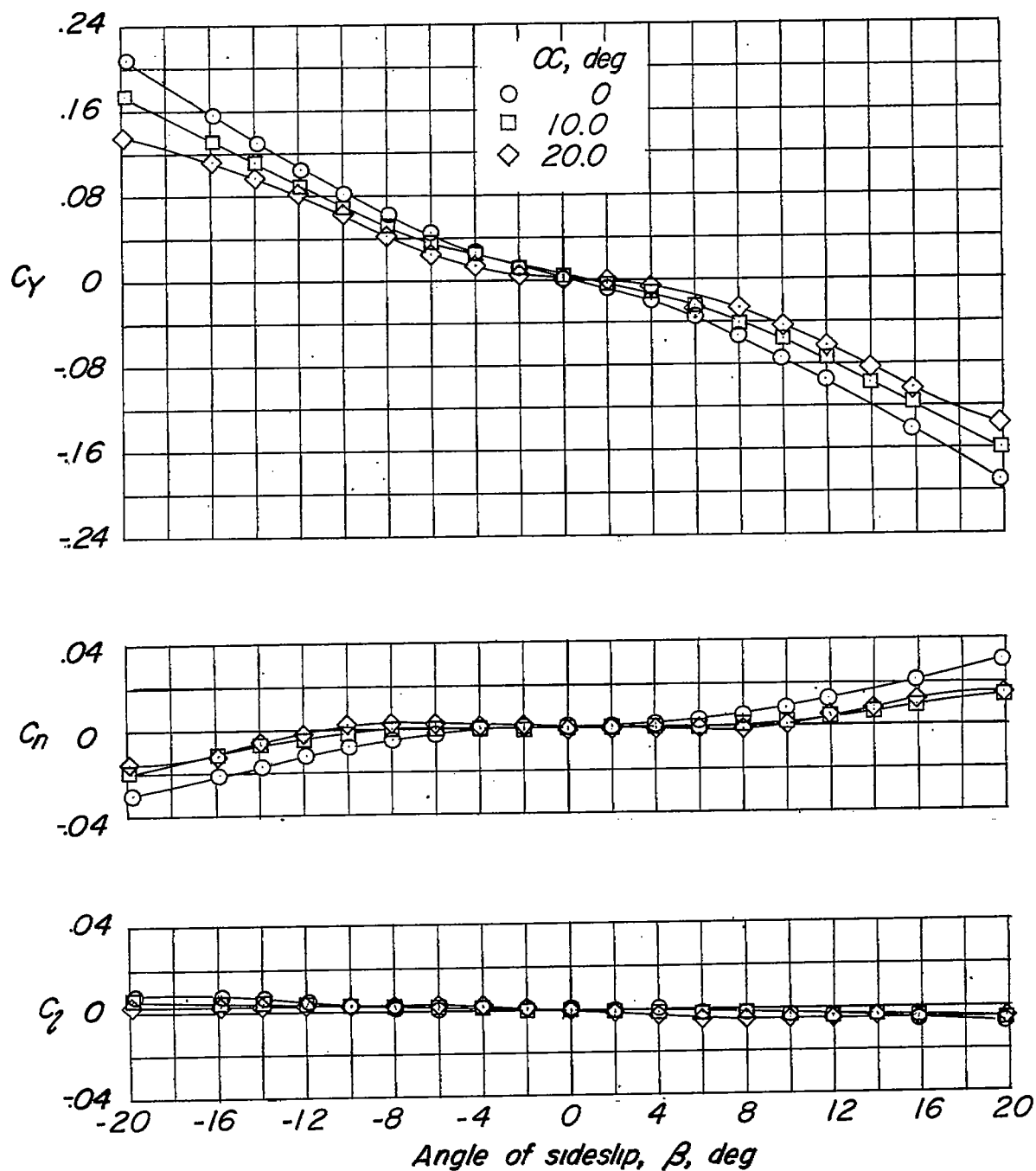$A_W = 4$.
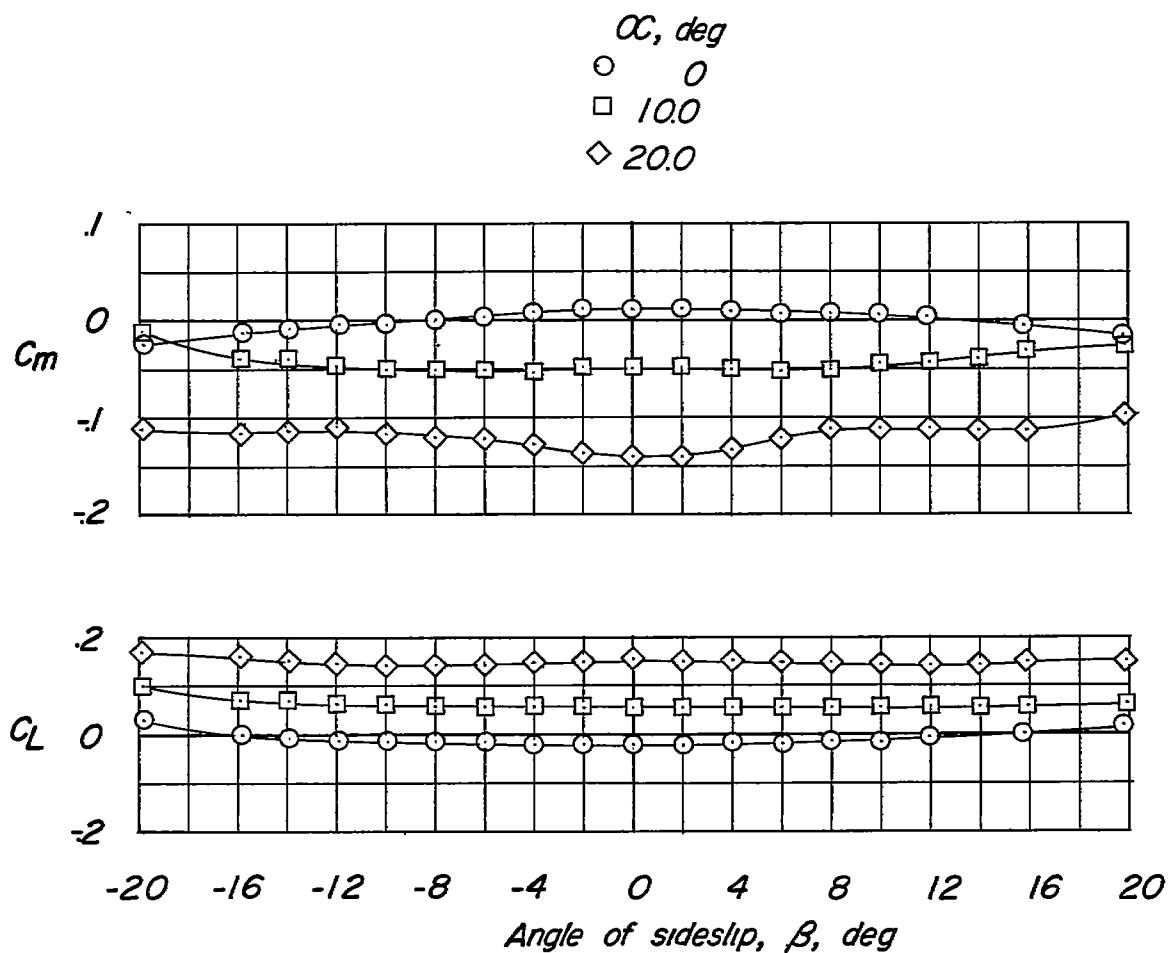
Figure 10.- Variation of C_L and C_m with β for the fuselage-tail combination. Coefficients based on aspect-ratio-4 wing.
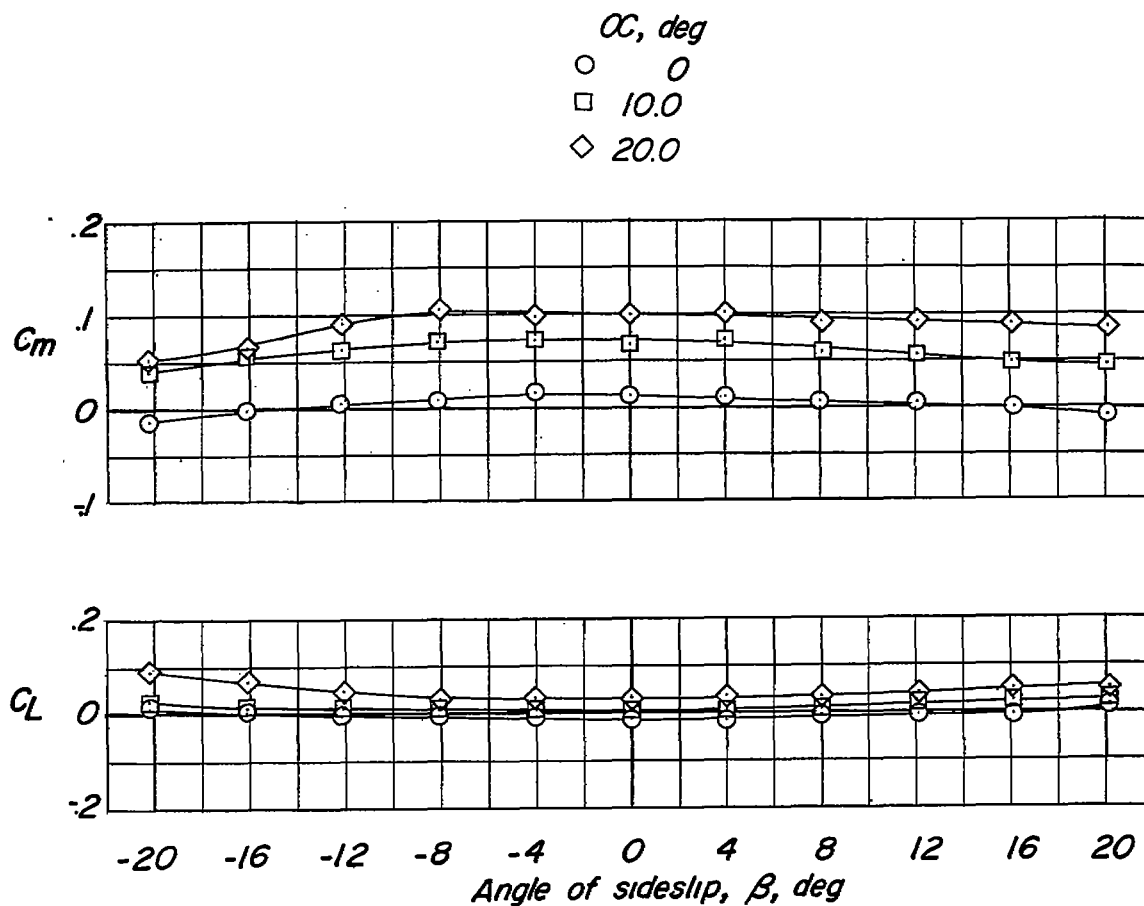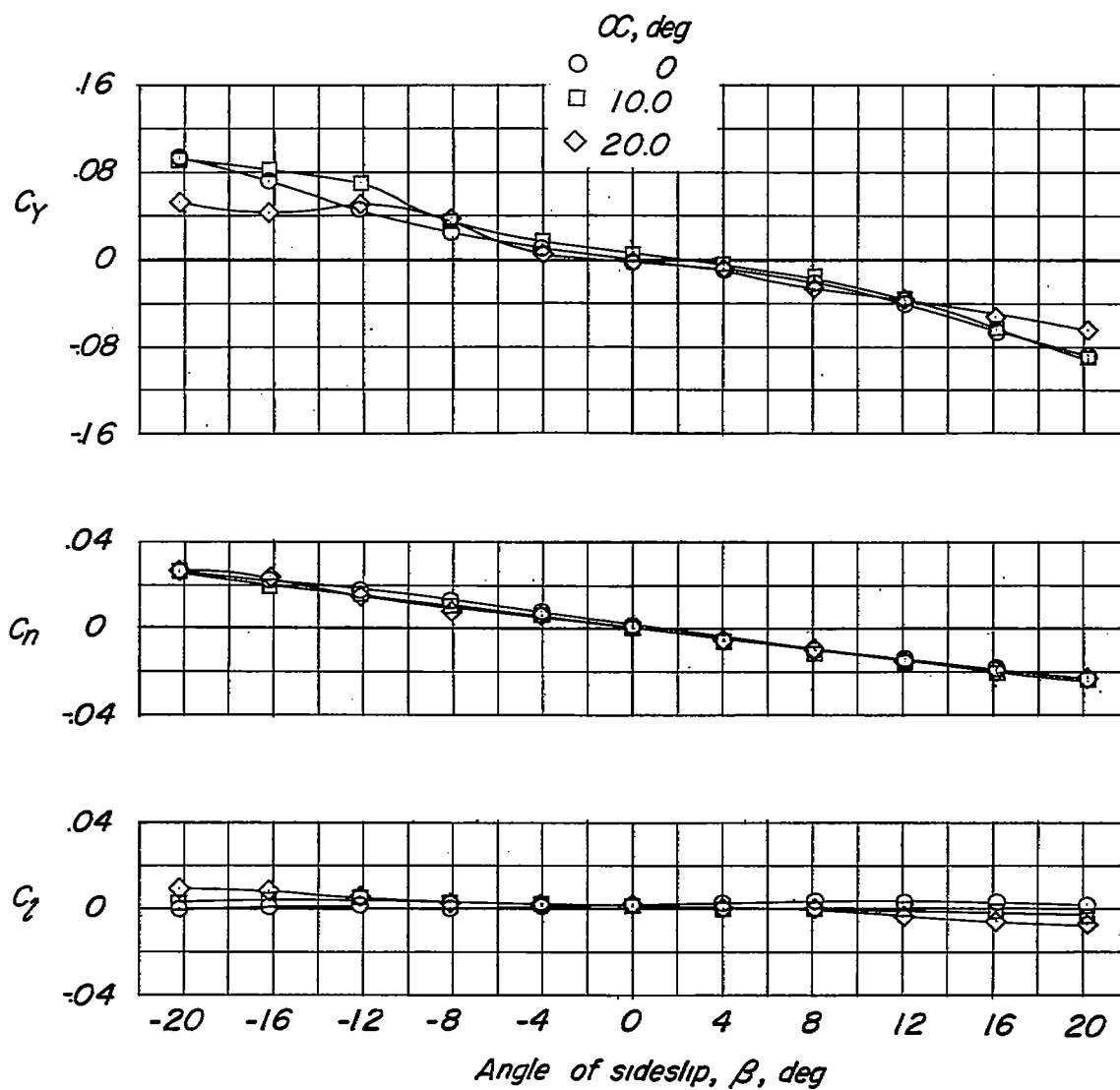
Figure 11.- Variation of C_L and C_m with β for the fuselage alone.
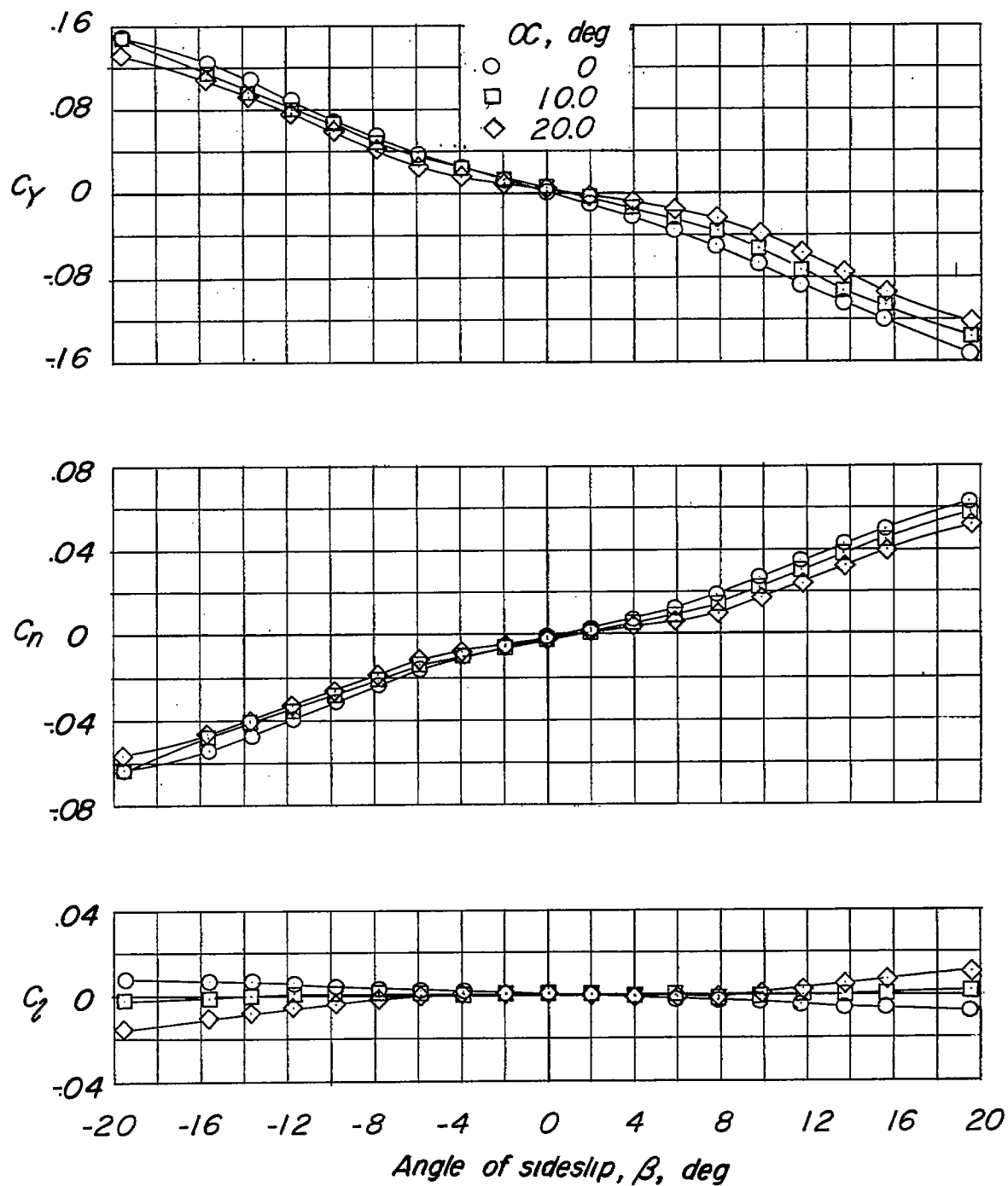Coefficients based on aspect-ratio-4 wing.
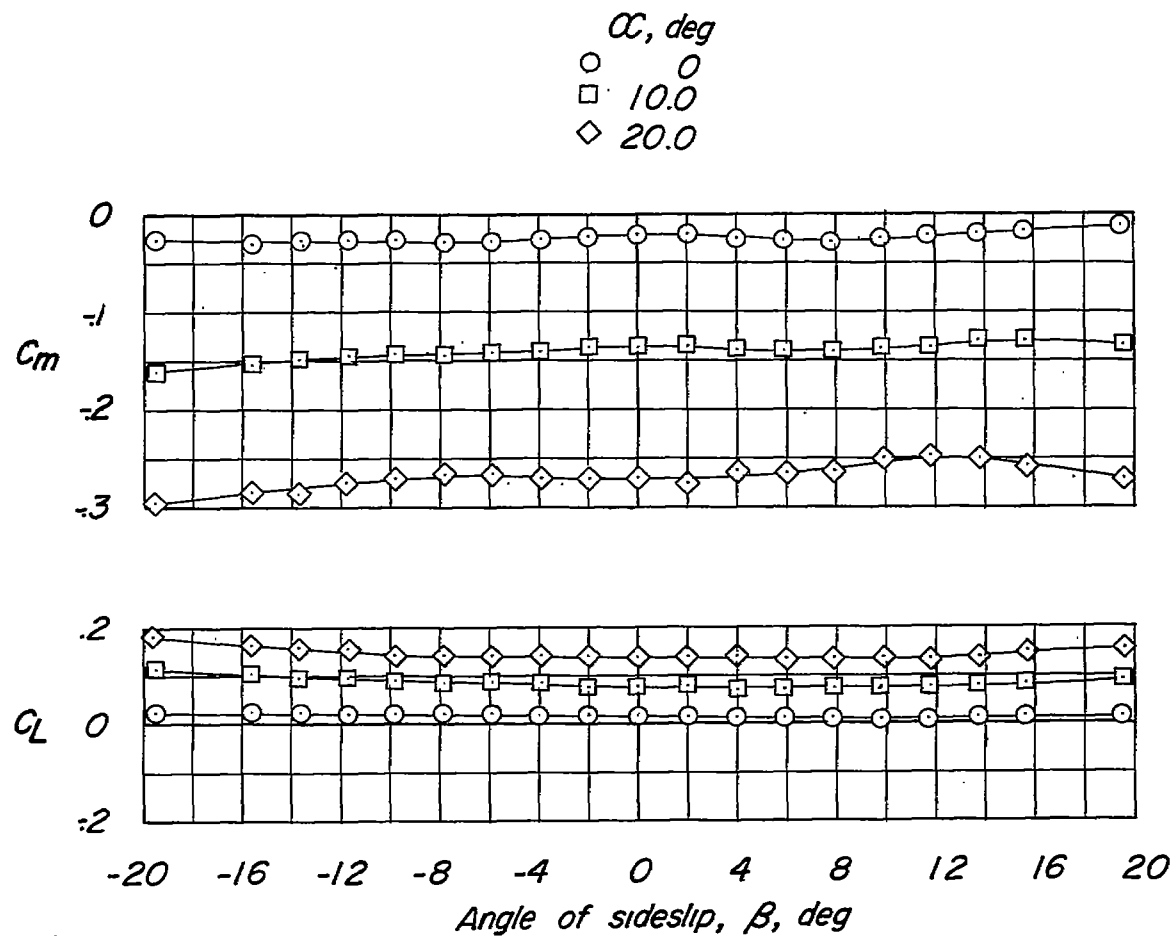
Figure 12.- Variation of C_L and C_m with β for the tail alone. Coefficients based on aspect-ratio-4 wing.
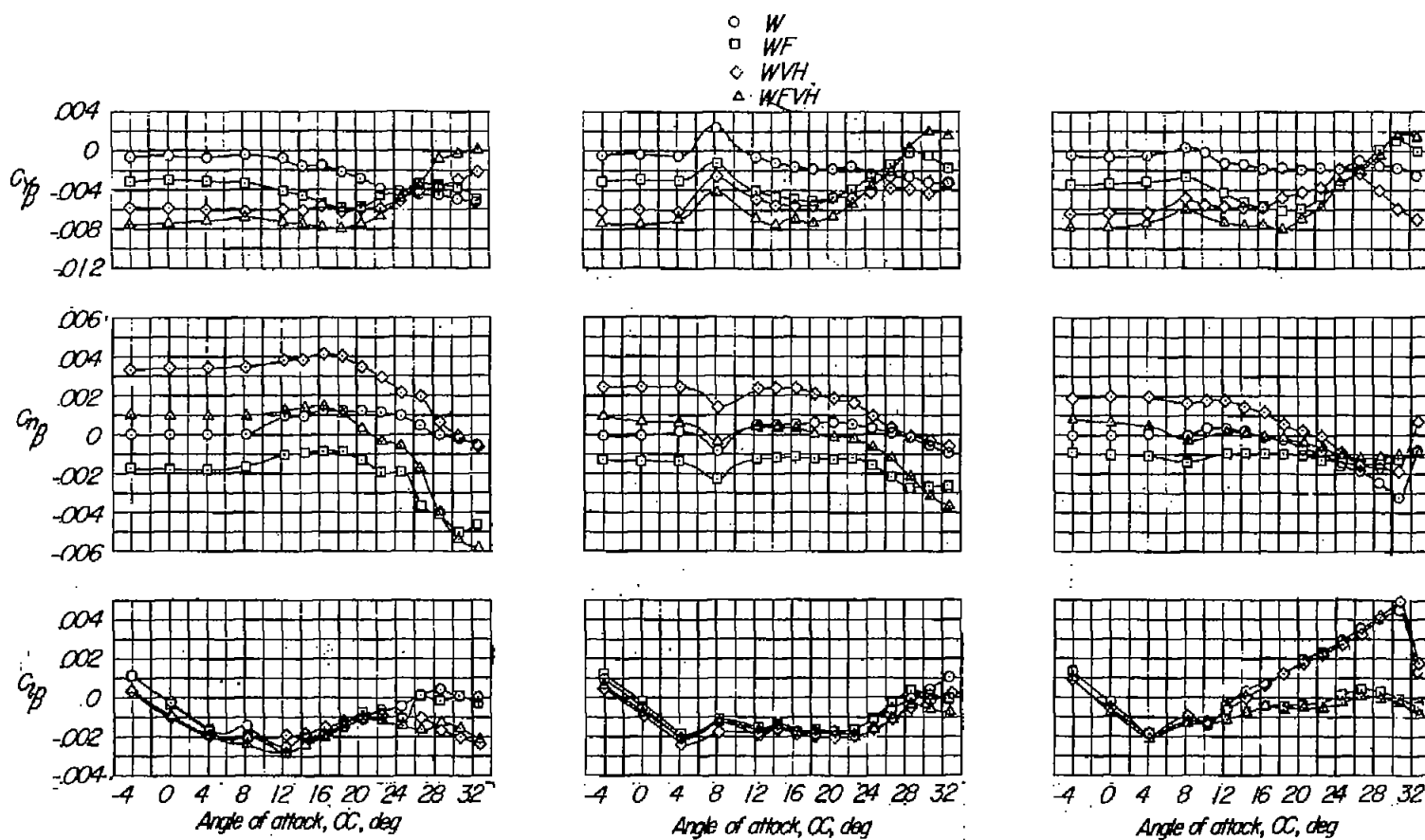
(a) Aspect-ratio-2 wing. (b) Aspect-ratio-4 wing. (c) Aspect-ratio-6 wing.

Figure 13.- Static lateral stability characteristics of the wing alone and in various combinations with the fuselage and tails.
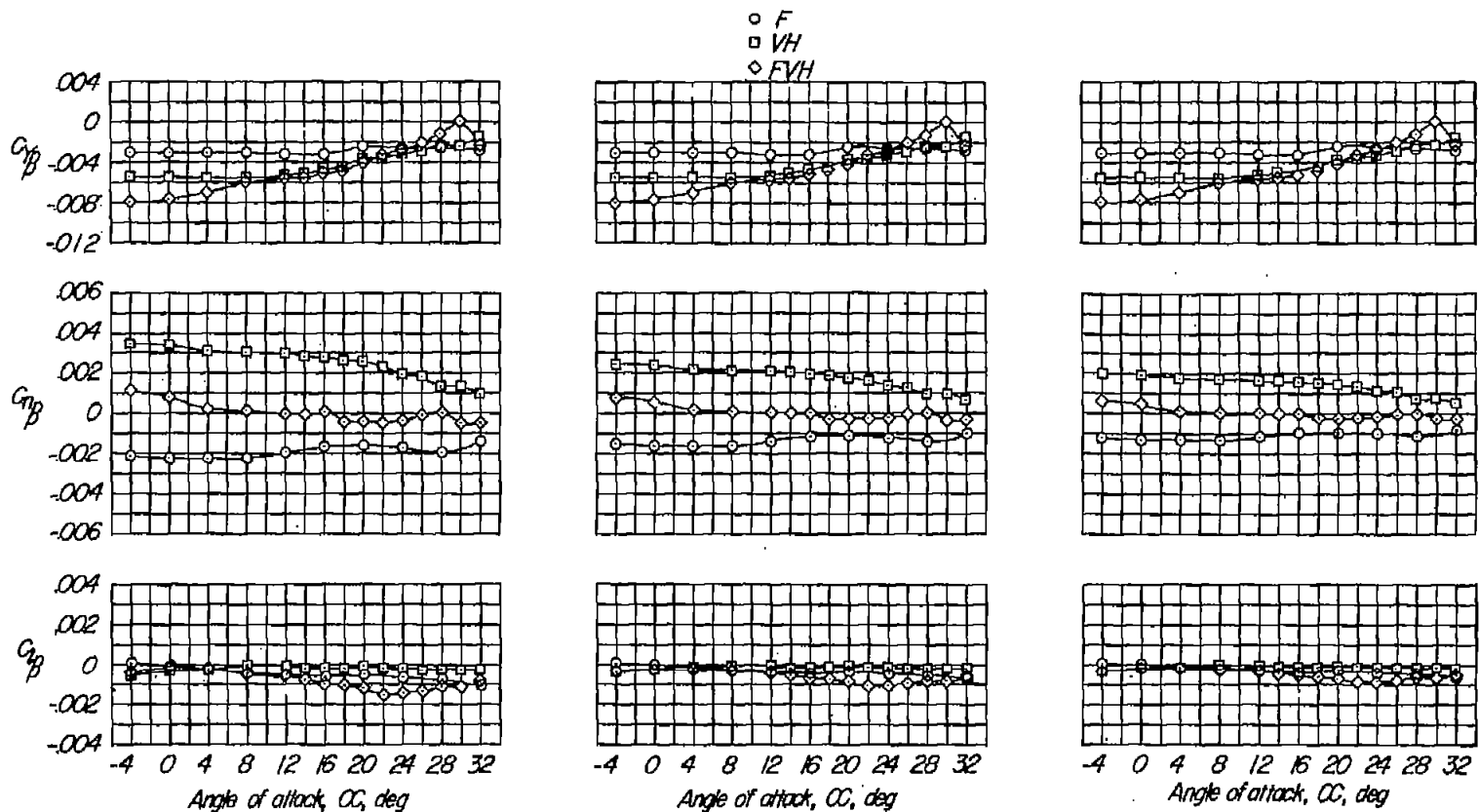
(a) Coefficients based on
aspect-ratio-2 wing.

(b) Coefficients based on
aspect-ratio-4 wing.

(c) Coefficients based on
aspect-ratio-6 wing.

Figure 14.- Static lateral stability characteristics of the fuselage alone, tail alone, and
fuselage-tail combination.
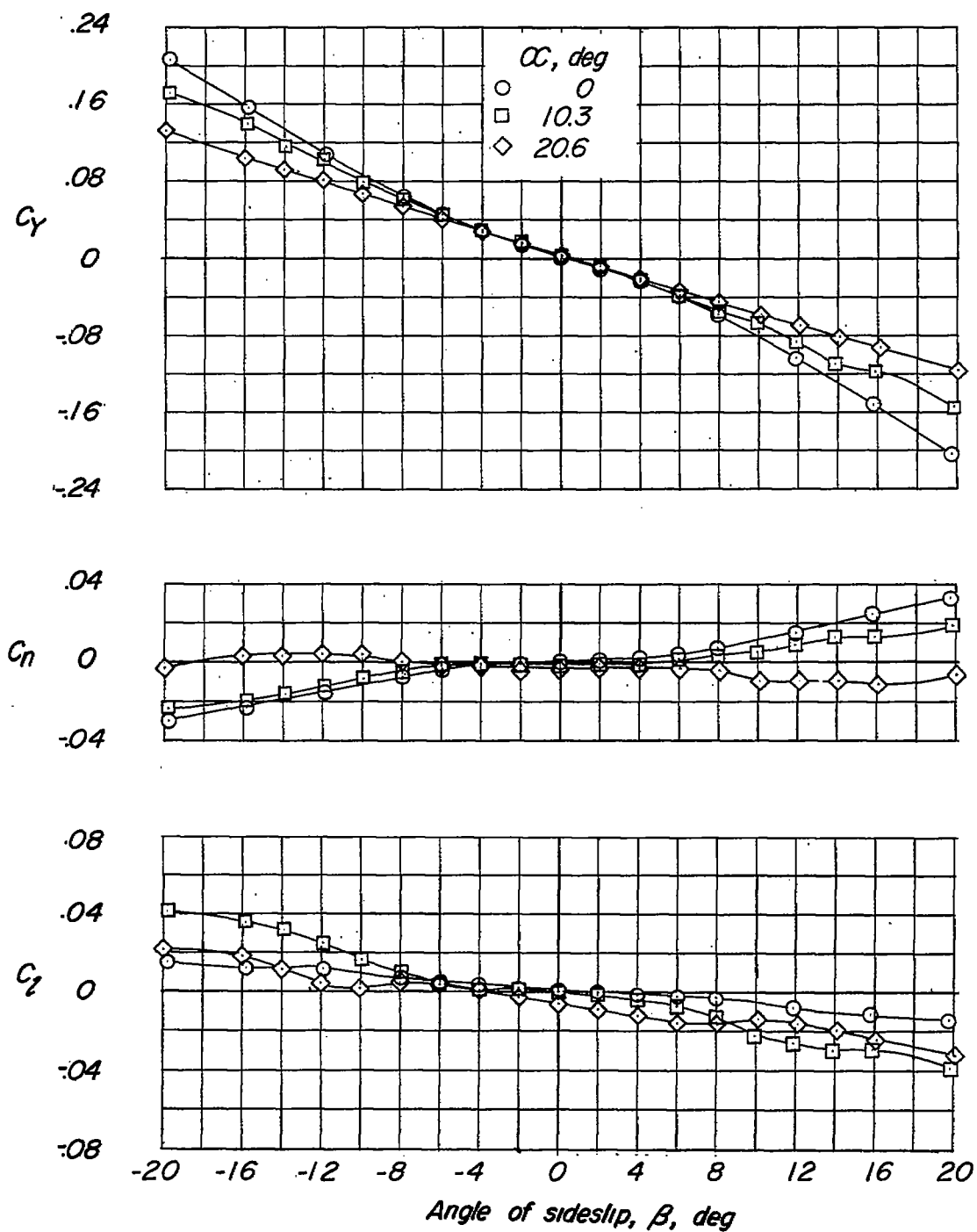
Figure 15.- Variation of C_Y, C_n, and C_l with β for the complete model. $A_w = 4$.

Figure 16.- Variation of C_Y, C_n, and C_l with β for the wing-fuselage combination. $A_w = 4$.
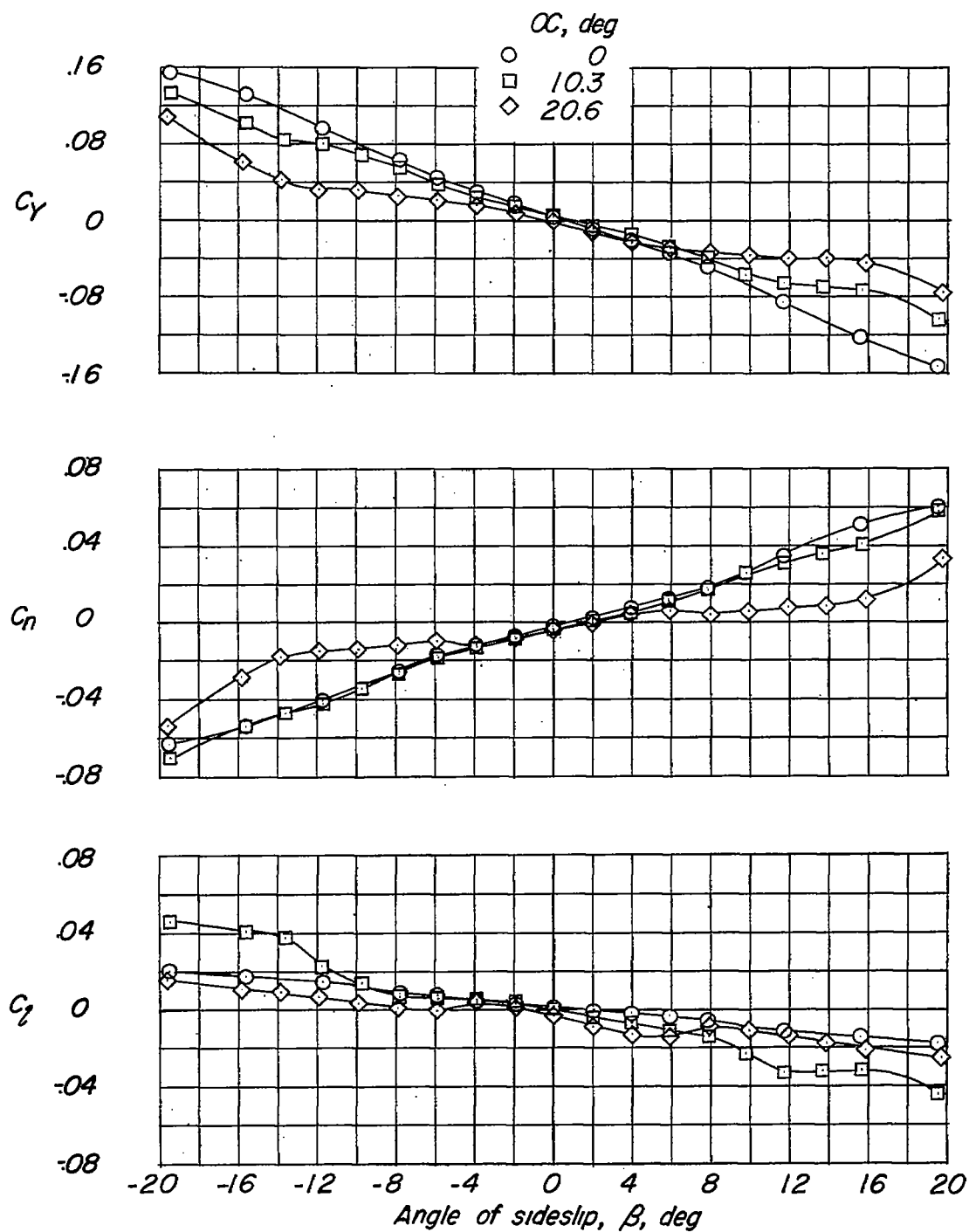
Figure 17.- Variation of C_Y, C_n, and C_l with β for the wing-tail combination. $A_W = 4$.
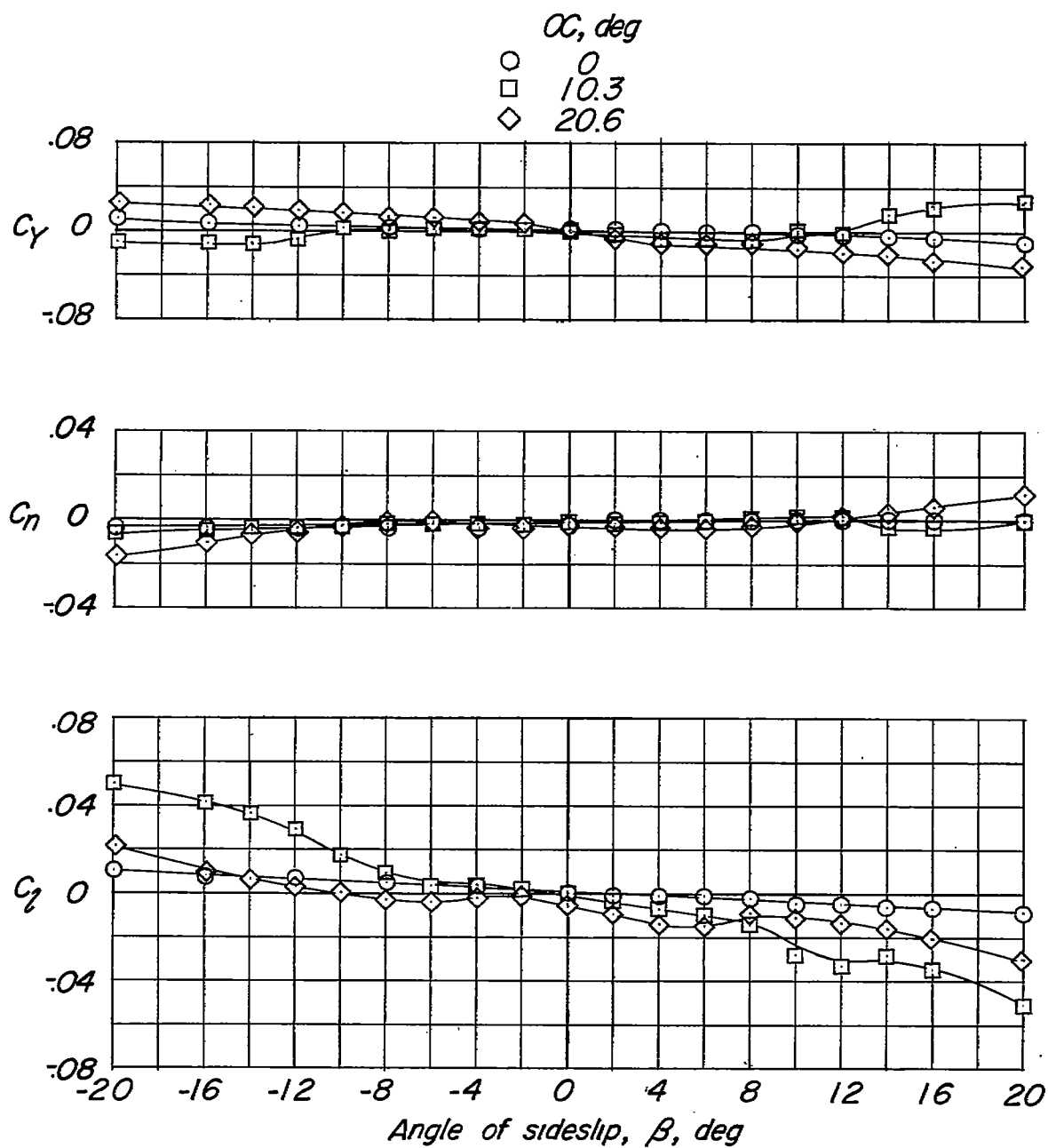
Figure 18.- Variation of C_Y, C_n, and C_l with β for the wing alone.
$A_W = 4$.

Figure 19.- Variation of C_Y, C_n, and C_l with β for the fuselage-tail combination. Coefficients based on aspect-ratio-4 wing.

Figure 20.- Variation of C_Y, C_n, and C_l with β for the fuselage alone. Coefficients based on aspect-ratio-4 wing.

Figure 21.- Variation of C_Y, C_n, and C_l with β for the tail alone. Coefficients based on aspect-ratio-4 wing.
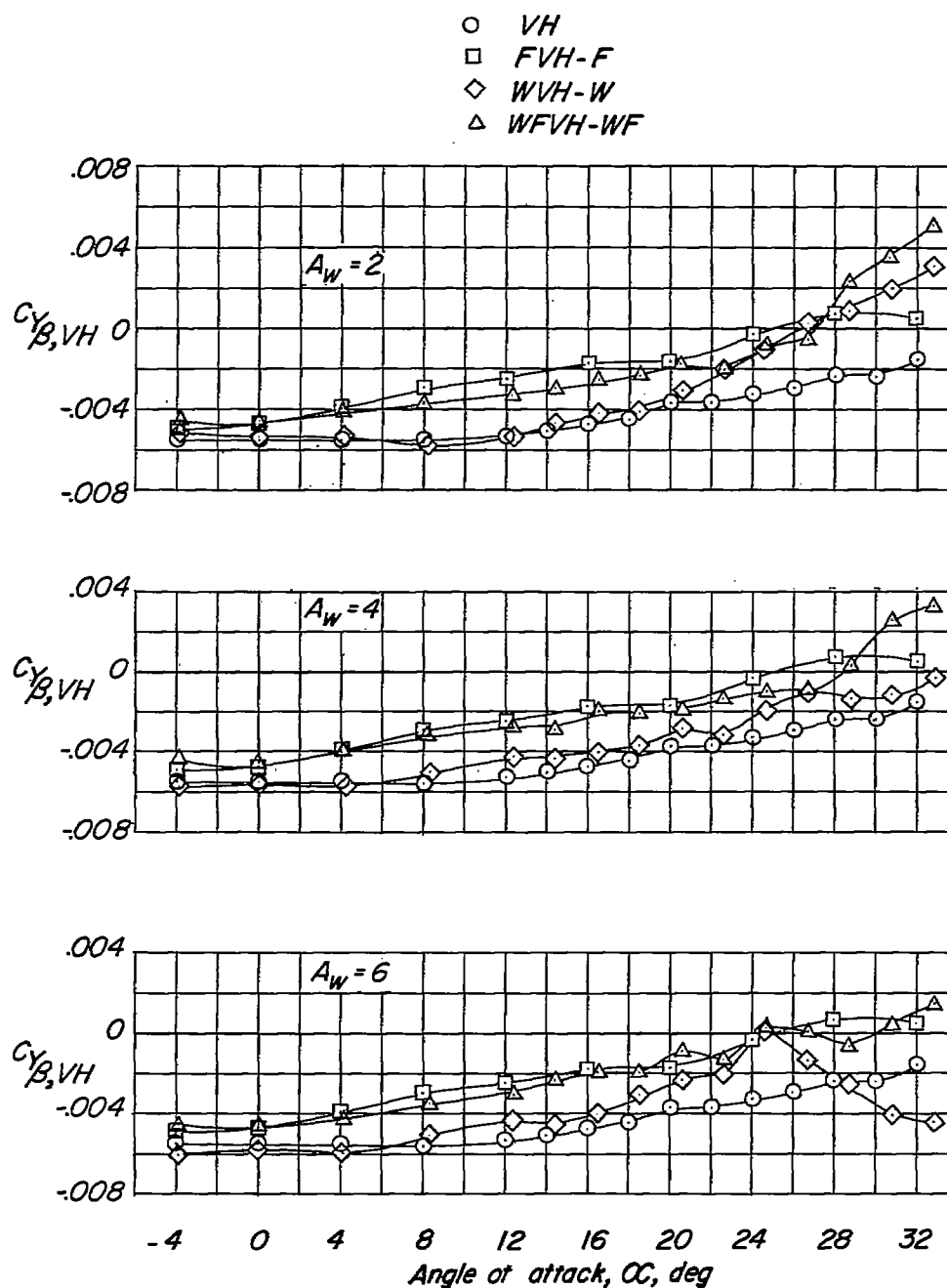
(a) Variation of $C_{Y_\beta,VH}$ with α.

Figure 22.- Effect of the various components on the tail contribution to the static lateral stability derivatives.
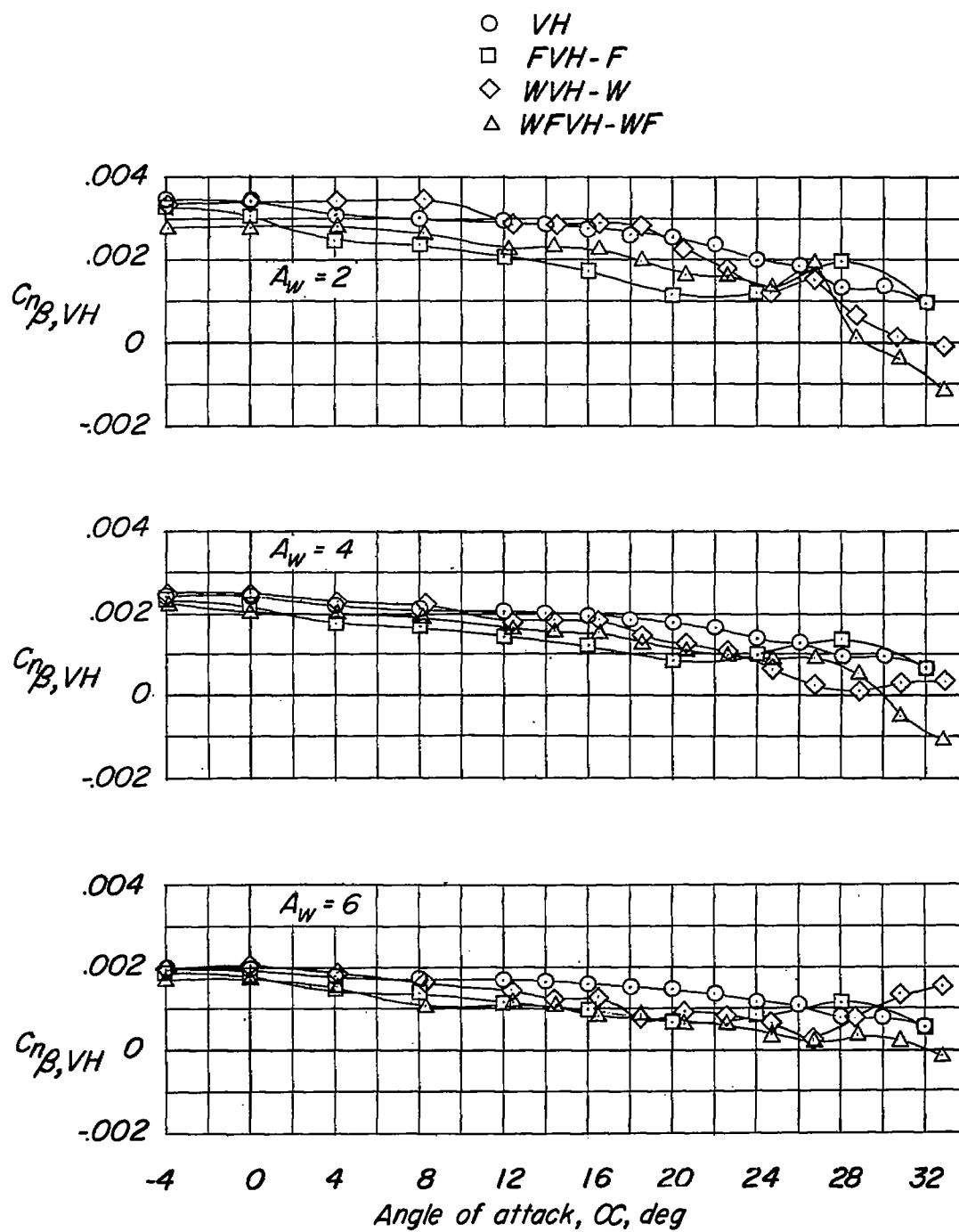
(b) Variation of $C_{n_\beta,VH}$ with α.

Figure 22.- Continued.
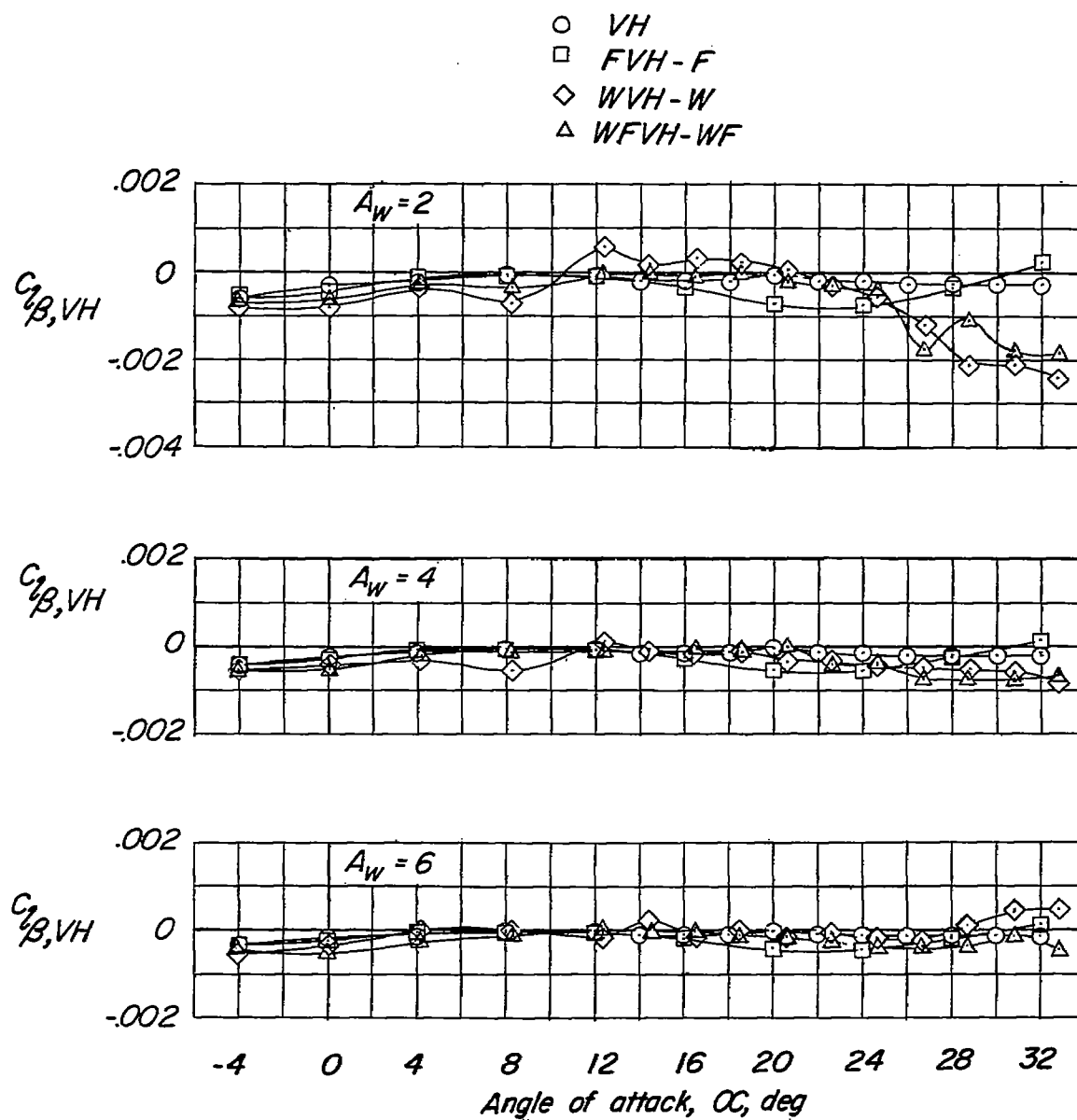
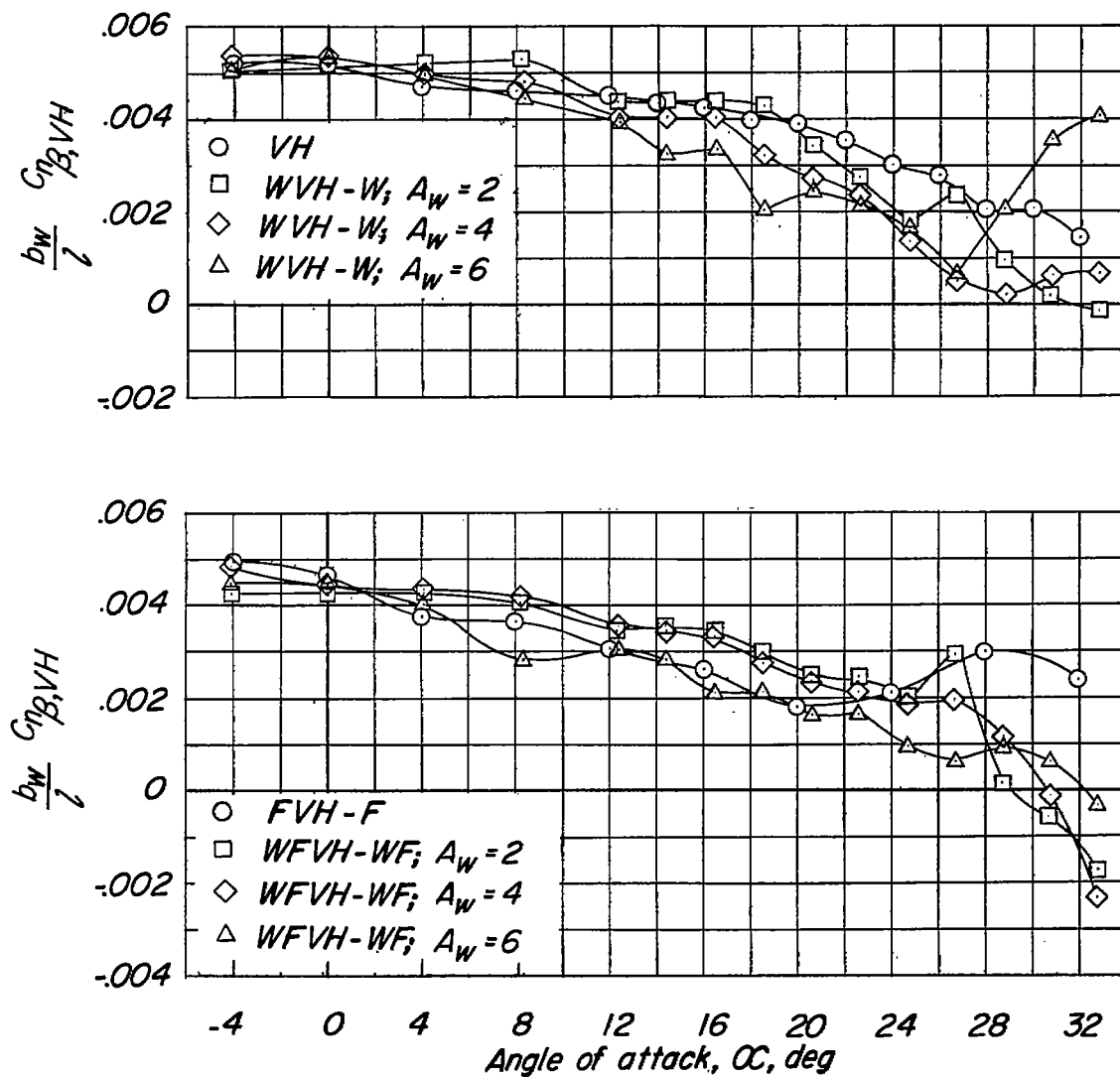(c) Variation of $C_{l_{\beta},VH}$ with α.
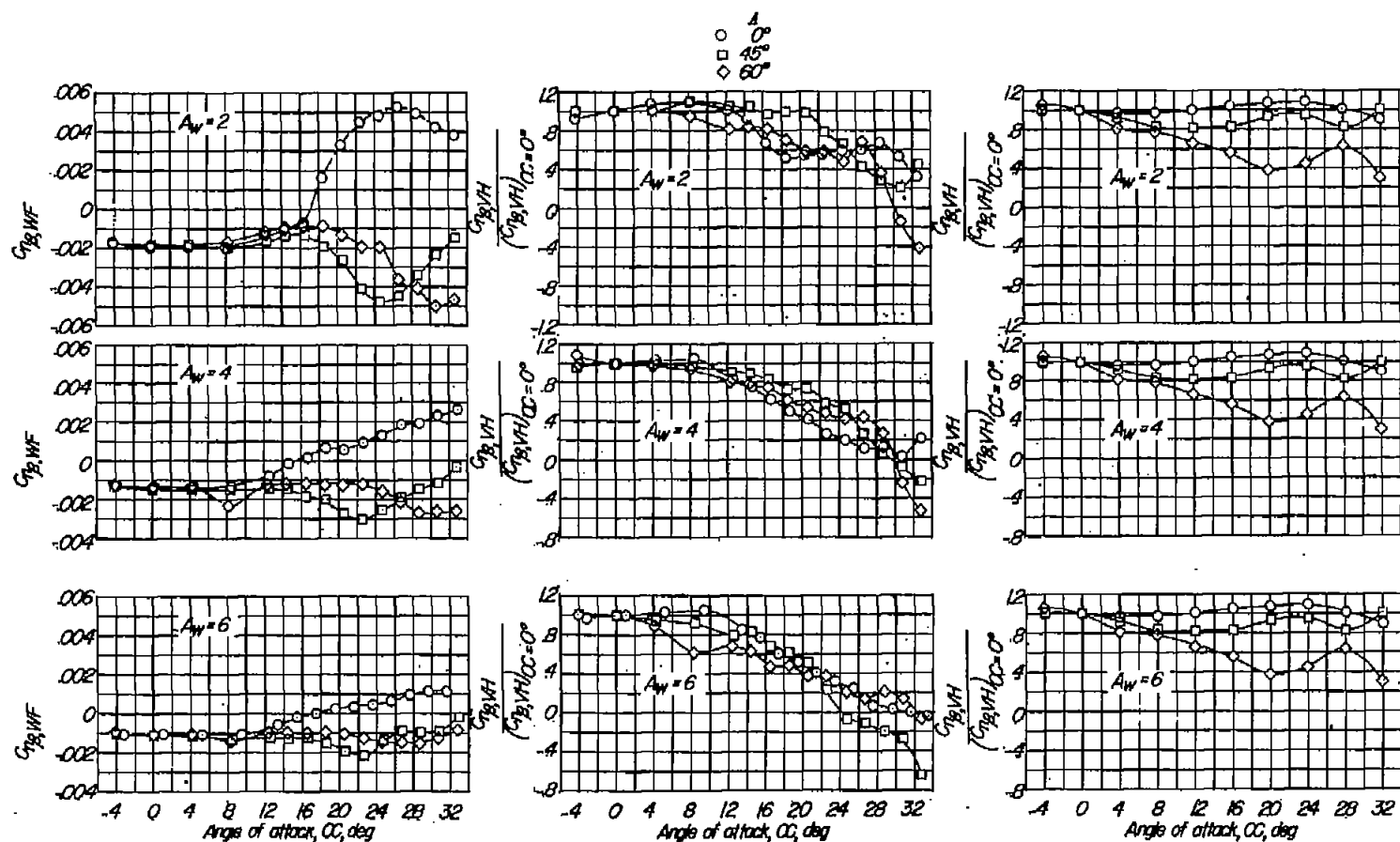
Figure 22.- Concluded.

Figure 23.- Effect of wing aspect ratio on the variation of $\frac{b_W}{l} c_{n_\beta,VH}$ with α.

(a) Wing-fuselage contribution to directional stability.

(b) Rate of change of tail effectiveness with angle of attack for the complete model.

(c) Rate of change of tail effectiveness with angle of attack for the fuselage-tail combination.

Figure 24.- The effects of wing sweepback on directional stability.